SEDIMENTOLOGY the journal of the International Association of Sedimentologists

Sedimentology (2021) **68**, 1698–1727 doi: 10.1111/sed.12859

The supercritical question for pyroclastic dune bedforms: An overview

GUILHEM AMIN DOUILLET*,† 

*Earth and Environmental Sciences, Ludwig-Maximilians-Universität München, Theresienstrasse 41, München 80333, Germany

†Institut für Geologie, Universität Bern, Baltzerstrasse 1+3, Bern, CH 3012, Switzerland (E-mail: guilhem.douillet@geo.unibe.ch)

Associate Editor – Dario Ventra

ABSTRACT

Sedimentary structures deposited from dilute pyroclastic currents are largely dominated by the products of metre-scale dune bedforms containing backset lamination. Since the first seminal works in the 1970s, the vast majority of the literature called these structures antidunes and chutes-and-pools. This consensus led to a loose terminology, either as descriptive terms for structures containing backset beds or as an interpretation of hydrodynamic conditions related to Froude-supercritical flows. Here, the main characteristics of pyroclastic dune bedforms are summarized and classified under four categories. The literature is examined and a discussion is provided regarding a possible interpretation in terms of supercritical-flow bedforms, including antidunes, chutes-and-pools and cyclic steps. The interpretation of pyroclastic dune bedforms as related to supercritical conditions is a possibility among others, yet open questions remain, and under the present state of knowledge alternative interpretations are equally valid. There is consensus that an interpretation of pyroclastic dune bedforms as related to supercritical flows implies deposition from a basal underflow supporting an internal free-surface formed at a density interface within the overall current structure. Antidunes are likely to be limited to low-angle, incipient bedforms. Chutes-and-pools may occur in the form of series of steep truncations formed by an erosive supercritical 'chute', with a depositional signature occurring exclusively in the subcritical 'pool' of a Froude jump. Rare examples of cyclic steps may be found as large-scale undulations with superimposed metre-scale bedforms, or for short-scale, fully-aggrading structures in periodic trains. Additionally, some pyroclastic bedforms may be formed by granular flows passing granular Froude jumps or as frozen granular stationary waves. The dominance of chute-and-pool structures over bedforms characterized by relatively more stable morphodynamics (antidunes and cyclic steps) could be the likely result of pulsating flow conditions and abrupt high-rate deposition, impeding stable flow conditions. In a majority of cases, the growth of pyroclastic bedforms appears triggered by the influence of an inherited bed topography and by bed-flow feedback effects. Apart from a possible interpretation as supercritical bedforms, other specific dynamics of dilute pyroclastic currents may well explain the characteristics of pyroclastic dune bedform structures. In particular, the inherent turbulence fluctuations, internal organization and highly depositional dynamics may be key to the formation of pyroclastic dune bedforms. In this respect, rather than solely focusing on the Froude dimensionless number of the formative current, theoretical considerations accounting for the Reynolds, Richardson and Rouse

dimensionless parameters may be also implemented for the understanding of pyroclastic bedforms.

Keywords Antidune, chute-and-pool, cyclic-step, dune bedform, pyroclastic, pyroclastic density currents, supercritical.

INTRODUCTION

Dilute pyroclastic currents

Pyroclastic currents – or Pyroclastic Density Currents (PDCs) – are ground-hugging flows made up of a mixture of pyroclasts comprising juvenile volcanic clasts and non-juvenile, entrained 'lithics' that are partly supported by a gas phase, mainly entrained air (e.g. Druitt, 1998; Burgisser *et al.,* 2005; Sulpizio & Dellino, 2008; Dufek, 2016; Lube *et al.,* 2020). Deposits from PDCs encompass a wide range of grain sizes from fine ash (silt size and below), coarse ash (any sand size), lapilli (granule and pebble size) or bombs/blocks (boulder size). A wide range of deposits is encountered spanning three end-members: massive, cross-stratified and draping, which are generally interpreted from a flow-bed boundary perspective as the products of dominant granular, traction or fallout processes, respectively (e.g. Wohletz, 1998; Branney & Kokelaar, 2002, chapter 4), or inertia-driven versus convection-driven flows (e.g. Doronzo & Dellino, 2014; Palladino, 2017).

Here, focus is on sedimentary facies associations containing dune-bedforms (DBs) cross-stratification and flow-oriented grain fabrics. These sediments are attributed to currents thought to have low particle concentrations, with clasts supported dominantly by fluid turbulence down to the flow base, and variously termed 'dilute PDCs', 'nuée ardente', 'ground surge' or 'pyroclastic surge' (e.g. Sparks & Walker, 1973; Sparks, 1976; Valentine, 1987; Branney & Kokelaar, 2002). Estimates of the higher limit of volumetric particle concentrations vary between authors, and could reach 2.8% by volume (e.g. Andrews & Manga, 2012; Weit *et al.,* 2018). Dilute PDCs are often an accompanying part of high concentration 'pyroclastic flows', with a range of allogenic and autogenic parameters influencing their interactions, such as: changes in the current density, temperature, momentum, source parameters and/or changes in slope along transport (e.g. Hoblitt, 1986; Burgisser & Bergantz, 2002; Doronzo & Dellino, 2014). Whereas a large portion of sediments from pyroclastic currents are massive and coarse-grained, ash-dominated and dune-bedded deposits have attracted attention since dilute currents have the capability to overflow topography through flow-stripping from concentrated flows (flow transformation or flow detachment, e.g. Hoblitt, 1986; Wohletz, 1998; Cole *et al.,* 2002; Douillet *et al.,* 2013a).

Here, an overview of the different types of dune bedforms and their interpretation in terms of Froude-supercritical flows is presented and discussed. Not considered here are bedforms related to secondary reworking by aeolian, fluvial or subaqueous processes (e.g. Suthren, 1985; Smith & Katzman, 1991; Manville *et al.,* 2009), extra-terrestrial environments, or subaqueous PDCs (e.g. Mandeville *et al.,* 1996; Pope *et al.,* 2018), although these structures can show some similarities to (Wilson & Hildreth, 1998; Burt *et al.,* 2008), and sometimes be confused with, primary deposits (Nocita, 1988, commented by McPherson *et al.,* 1989). This work is justified by two motivations: (i) The understanding of pyroclastic DBs has the possibility to deliver crucial insights into the dynamics of dilute PDCs. (ii) Conversely, the particular sedimentary environment represented by PDCs provide unique information for the field of process sedimentology.

The specificities of dilute pyroclastic density currents

The sedimentary record of dilute PDCs is in many ways atypical compared to that of most sedimentary environments, and may capture processes that are only transient in aqueous or wind-driven transport (e.g. Wohletz, 1998; Burgisser *et al.,* 2005). In order to understand this uniqueness, the introduction of dimensionless numbers permits the evaluation and comparison of different types of flows in a unified framework (definitions in Table 1). Hypotheses on the flow characteristics of PDCs can be formulated to explain the specificities found in their deposits:

1 Pyroclastic density currents are a form of particulate density currents, i.e. a flow where particles at relatively high concentration constitute the current and drive its motion under the direct

Table 1. Overview of the dimensionless numbers and physical quantities listed in the manuscript: u = flow velocity; g = gravity acceleration; g' = reduced gravity; H = characteristic length (here flow thickness); ρ = flow density; L = characteristic length (particle diameter/flow thickness); μ = dynamic viscosity; d/dz is the derivative to height; w_s = fall velocity of particle; K = Von Karman constant, δ = characteristic length (of turbulence); f = frequency of vortex emission; L is a characteristic length (e.g. flow thickness); ρ_0 = bulk flow density.

	Symbol	Definition	Formula for flows
Dimensionless numbers			
(Densimetric) Froude number	$Fr_{(d)}$	Ratio of inertia to external forces - generally gravity	Here, $Fr = u/(g' * H)$
(Particle) Reynolds number	Re	Ratio of inertial to viscous forces	$Re = \rho * u * L/\mu$
Richardson gradient number	Ri	Ratio of buoyancy to shear/turbulent mixing	$Ri = N^2/(du/dz)^2$
Rouse number	P	Ratio between particle settling velocity and scale of turbulence	$P = w_s/(K * u^{*)}$
Stokes number	St	Decoupling of particle regarding turbulence (there exist various formulations depending on flow configuration)	$St = w_s * u^*/\delta g$
Strouhal number	Str	Ratio of inertial forces due to local acceleration (i.e. evolving through time) to the ones due to advected acceleration (i.e. carried with a fluid parcel)	$Str = f * L/u$
Other quantities			
Brunt-Vaisala (or buoyancy) Frequency	N	Measure of the stability of flow-stratification. The free oscillation frequency of a fluid interface	$N = (-g/\rho_0 * d\rho(z)/dz)^{0.5}$
Shear (or friction) velocity	u*	A measure of flow shearing with dimension of a velocity	Slope of the logarithmic velocity profile

effect of gravity. Here the role of particles stands in fundamental contrast to aeolian or fluvial transport, where the fluid phase is set in motion by gravity, independent of its associated particulate load, and can secondarily entrain and transport particles. Hence, in a particulate density current, the momentum (i.e. velocity * mass) is carried by the particle load. When particles are deposited, the flow mass decreases, and so does the momentum. Furthermore, particles are present throughout the flow's thickness and path, without the need of being picked up prior to deposition, resulting in a ubiquitous availability of particles, with material in the upper part of the current being able to feed an underflow (e.g. Gardner *et al.,* 2017). These characteristics are shared with all particulate density currents (for example, turbidity currents and snow avalanches).

2 The density ratio between the particles and the fluid phase (air) is much larger than for any water-supported transport process and the dynamic viscosity of air is two orders of magnitude lower (e.g. Burgisser *et al.,* 2005). Accordingly, the dynamics applying to pyroclastic currents might share little with water-supported sediment transport, and one must consider scaling laws embracing the Rouse and Stokes dimensionless number (Table 1; e.g. Valentine, 1987). This is a major divergence from subaqueous turbidity and hyperpycnal currents.

3 The combination of the availability of particles and their high density-contrast to the supporting fluid may lead to extreme sedimentary dynamics, in particular, through fast sedimentation and draping that may freeze processes otherwise not available in a 'regular' sedimentary record. The growth of some bedforms and associated sedimentary structures may take place within seconds to minutes.

4 The wide particle-size distribution within pyroclastic deposits is a token for the high polydispersity of the parent flows that emplaced these sediments. Polydispersity may be key in PDC dynamics and sedimentology. By fostering the entrapment of air and elevated interclast fluid pressures (pore pressure), polydispersity may facilitate the occurrence of a fluidized boundary-layer zone (e.g. Sparks, 1976; Druitt *et al.,* 2007;

Smith *et al.,* 2018; Breard *et al.,* 2018, 2019). In particular, dilute PDCs are likely to grow basal underflows dominated by a transitional layer of traction carpets, fluidized granular flows and metastable early sediment (e.g. Sheridan & Updike, 1975; Druitt, 1992; Sohn, 1997; Douillet *et al.,* 2015), as for turbidity currents (e.g. Sanders, 1960). In the quasi-absence of direct observations on the internal structure of dilute PDCs, their sedimentary signatures are the largest source of natural observation (exception: Scharff *et al.,* 2019).

Supercritical flows

A flow where more energy is stored as kinetic energy than potential energy is said to be in the Froude-supercritical regime, this relation being expressed by the dimensionless Froude number (Fr; Table 1) attaining values greater than unity. This regime is independent of the turbulent state of a flow (laminar versus turbulent, depending on Reynolds number, Re; Table 1), or of the total amount of energy stored in the flow. Sedimentary structures formed under critical to supercritical flow conditions are grouped under five types: upper-stage planed beds, antidunes, breaking antidunes, chutes-and-pools and cyclic steps (e.g. Simons *et al.,* 1961; Alexander *et al.,* 2001; Cartigny *et al.,* 2014).

The supercritical regime also corresponds to flow conditions where the current runs faster than the group-velocity of surface gravity waves propagating at its upper free boundary (respectively, subcritical, slower). When a current moves at similar speed as gravity waves (transcritical regime), upstream propagating surface waves appear to be almost stationary over the sediment bed, and may interact with the bed to form a bedform: an antidune (e.g. Gilbert, 1914; Kennedy, 1963). 'Antidune' is thus, from a sedimentology point of view, intrinsically interpretative and this term does not contain any descriptive connotation (see *Nomenclature* section for descriptive terms). One of the advantages of interpreting a sedimentary structure as originating from an antidune is that it allows to apply a simple equation frame to extract quantitative flow parameters. The rationale is that an antidune would be the mould of a stationary surface gravity wave in a current having a Froude number equal to or close to unity (e.g. Prave, 1990; for the complete development of the framework, see Douillet, 2015, chapter 2). Unfortunately, there has been a tendency in the literature to use the word antidune as a descriptive term.

In the supercritical regime, surface gravity waves are too slow to travel upstream in reference to the bed. Since gravity waves act as the agent of transfer for changes in flow depth, a supercritical flow cannot 'foresee' a change in height, as for example resulting from an obstacle or a dam (hence supercritical is also termed 'shooting'), whereas a subcritical flow does. The passage from super to subcritical can thus lead to an abrupt flow 'jamming', forming a so-called 'Froude jump'. Whereas the term 'hydraulic jump' is more commonly used for this phenomenon, the absence of water in a PDC is here considered an obvious reason to adopt the more generic term 'Froude jump' in this manuscript ('pneumatic jump' and 'granular jump' have also been used for pyroclastic currents; e.g. Branney & Kokelaar, 2002; Douillet *et al.,* 2013a, 2019; Smith *et al.,* 2020). Both sedimentation and/or erosion may occur (alone or concurrently) at a Froude jump, and may lead to the development of bed configuration known as a chute-and-pool (e.g. Jopling & Richardson, 1966). Just like 'antidune' specifically applies to a bedform related to a stationary gravity wave, the term 'chute-and-pool' is used for any bed configuration related to a Froude jump. Again, that term thus appears as solely interpretative from a sedimentological point of view, and does not contain descriptive sedimentary characteristics. When a flow develops a train of repetitive, long-wavelength Froude jumps, the corresponding bed configuration is called 'cyclic steps'.

Diversity of pyroclastic dune bedforms

Nomenclature

The term 'surge' is abundant in the literature, yet avoided here due to its potential ambiguity, since it refers both to a dilute PDC in volcanology and to a retreating Froude jump in hydrodynamics. The term 'dune bedform' (DB) refers to a roughly metre-scale bed undulation forming an individual sedimentary structure (or non-planar bedsets, Fig. 1). Here, DB is not restricted to a superficial shape but includes the stratification participating in the formation of the outer shape, i.e. the associated sedimentary structure (Fig. 1A; e.g. Carey, 1991; Douillet *et al.,* 2013). The stratal patterns record the succession of bed shapes with time. Dune bedform is preferred over the variety of other terms applying to the same objects because of its absence of genetic connotation, yet the pyroclastic literature abounds with such terms as 'wave', 'sandwave', 'megawave', 'wave-form',

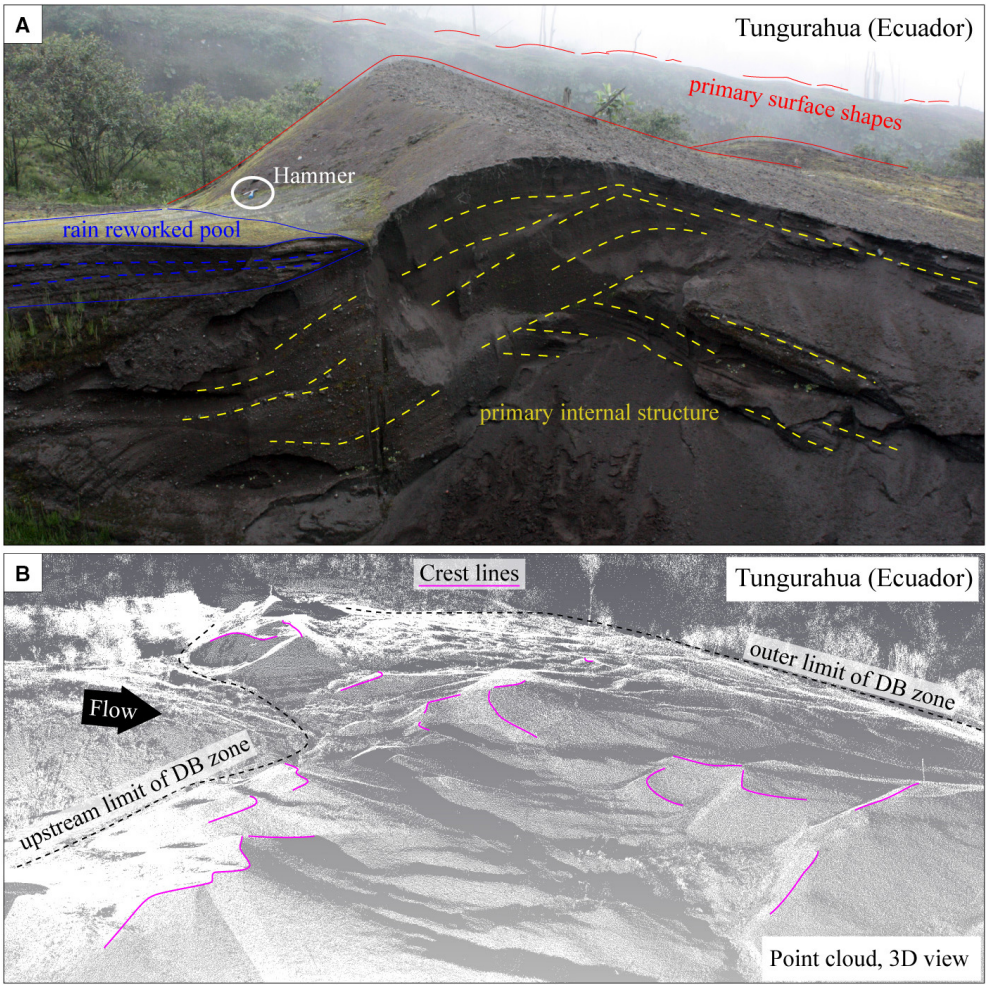

Fig. 1. For all illustrations in this article, flow direction approximately from left to right. Overview of dune-bedform (DB) deposition fields from the 2006 eruption of Tungurahua. (A) DB shape with internal sedimentary structure. Note field of DBs and still standing dead trees in background. Hammer for scale is 28.5 cm long. (B) Field of DBs in the proximal domain of a depositional zone, seen from a terrestrial laser scanner point cloud. Width of image is *ca* 40 m (Achupashal area; see Douillet *et al.,* 2013a,b).

'megaripple', 'dune', 'dune-like', 'antidune', 'bedform' or 'dune bedform'. The terms 'antidune' and 'chute-and-pool', which have been pervasively used as descriptive terms by volcanologists, are reserved here to their hydrodynamics meaning only (see above).

Deposits with stratification include any type of strata, including 'laminations' used for millimetre-scale strata, whereas 'layers' are massive, pluri-centimetric thick strata. A 'laminaset' is a set of several laminae forming a consistent pattern, intrinsically understood as related to a single accretion phase; laminasets are separated by set boundaries, either erosive or conformable (stratasets refer similarly to groups of strata). 'Cross-stratification' is used with general reference to any strataset with angular relationship with respect to its bounding surface. The 'stoss' face of a bedform faces upstream, and the 'lee' faces downstream. Stratasets deposited on a stoss side are called 'backsets' (not to be confounded with 'backsteps', which correspond to a stratigraphic transgressive stratal architecture pattern), as opposed to the term 'foresets', denoting stratasets dipping downcurrent along a bedform lee side. Stratasets that show continuous deposition from the stoss to the lee side are called 'fully-aggrading'. Fully-aggrading stratasets that show thicker strata toward their stoss entail a general upstream shift of the bedform crest and are called 'regressive', whereas stratasets with a downflow equivalent trend are called 'progressive'.

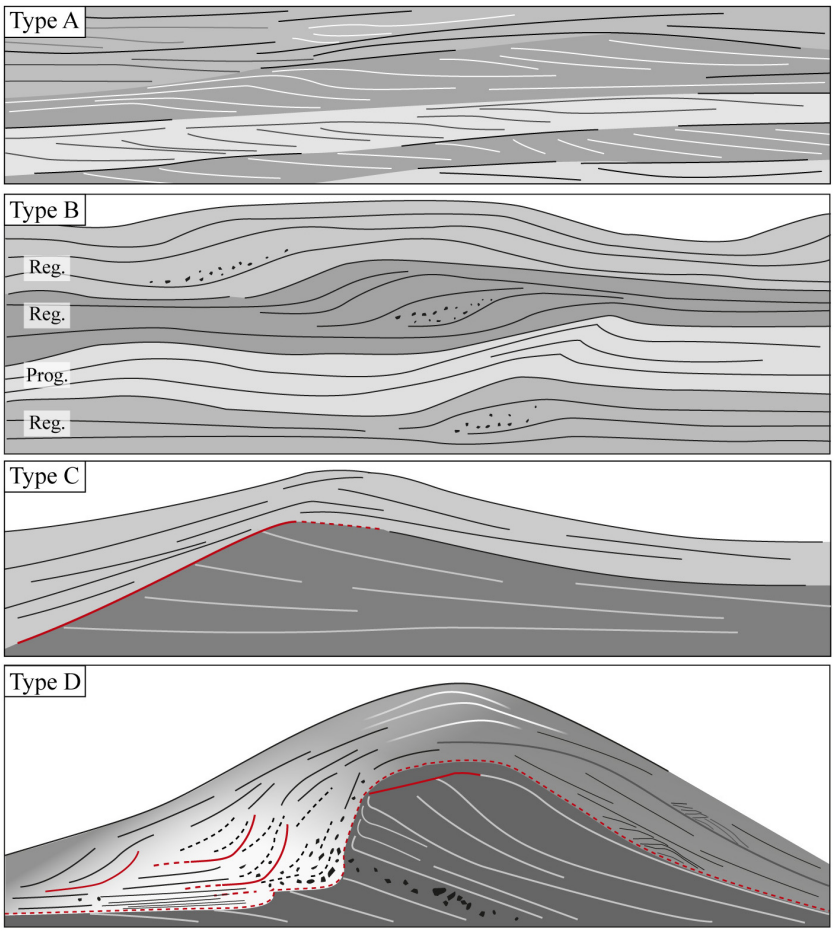

Fig. 2. Schematic representations of the four end-member types of pyroclastic dune-bedforms identified here. (A) Low-angle structures. (B) Fully-aggrading structures of progressive (prog.) or regressive (reg.) nature. (C) Truncated structure with covering beds. (D) Steep truncations covered by high-angle backset beds. For all illustrations, flow orientation roughly from left to right.

Structural characteristics

Primary pyroclastic DBs have been documented in the past and present with consistent descriptions of a variety of typical structural characteristics, including (Figs 1 and 2):

- Sedimentary structures from DBs preserved as individual bedforms with a clear stoss and lee side. This 'formset' organization is the most distinctive characteristic, with only sporadic counterexamples of tabular sets (e.g. Sohn & Chough, 1989);
- Widespread occurrence of backset strata, with dip angles varying from sub-planar to vertical (e.g. Schmincke *et al.,* 1973; Douillet *et al.,* 2019);
- Truncation events are mainly visible on the stoss sides of DB structures (e.g. Moore *et al.,* 1966; Moore, 1967; Schmincke *et al.,* 1973; Tokunaga & Yokoyama, 1979; Bestland & Krull, 1999; Brand *et al.,* 2016; Douillet *et al.,* 2019). These range from sub-horizontal to vertical. Uncommon studies have reported lee side erosion, which might be an interpretation bias (Belousov & Belousova, 2001);
- Stoss sides are generally steeper than lee sides (e.g. Moore, 1967; Rowley *et al.,* 1985; Belousov & Belousova, 2001; Douillet *et al.,* 2013b);
- Widespread occurrence of fully-aggrading structures with progressive to regressive nature.
- Common co-existence of peculiar finer-scale structures (Fig. 3; Douillet *et al.,* 2015, 2018, 2019, and references therein) such as:

  - lineations (i.e. non-massive deposits with coherent lines that cannot confidently be attributed to depositional laminae);
  - shark fins (Fig. 3A, i.e. centimetre-scale overturned flame structures) in zones of low-angle erosion with lineations;
  - vertical truncations covered with lineations (Fig. 3B);
  - overturning truncations (Fig. 3C, i.e. a truncation plane underlined by a zone of overturned laminae);

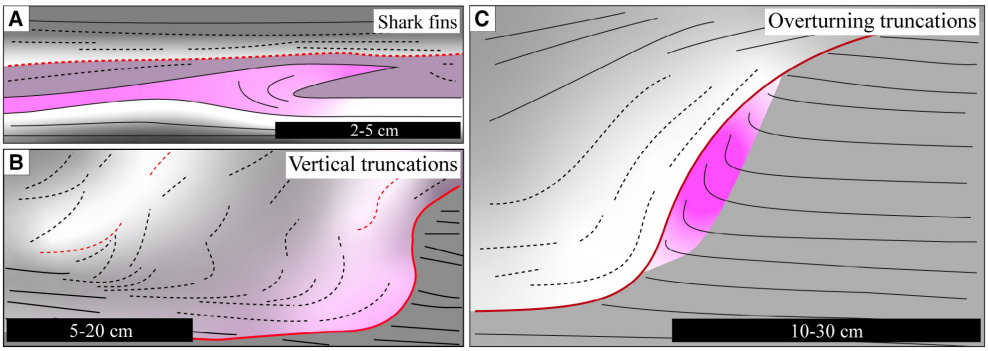

Fig. 3. Small-scale features common in pyroclastic dune-bedform structures. (A) 'Shark fins' are flames overturned in the flow direction. (B) Vertical truncations commonly covered by lineated to massive beds. (C) Overturning truncations, whereby the laminae directly underlining a steep truncations are consistently overturned with a shift and depth of a few centimetres. These features are consistent over a distance of a few to tens of centimetres. Laminae are denoted by solid black lines, erosion surfaces by solid red lines, lineations by dashed lines. For all illustrations, flow orientation roughly from left to right.

- backset ripples (Fig. 6B, i.e. ripple sized, fully-aggrading, regressive structures).

These structures are generally attributed to a combination of high sedimentation rates, high bedload with granular-based flows and traction carpets, and metastable sediments during the early phase of deposition.

The quasi absence of ripples with preferential downstream aggradation (i.e. with exclusion of 'backset ripples') is characteristic of the depositional environment of pyroclastic DBs. Rare reported occurrences might be an exception (e.g. Dellino & Volpe, 2000), yet often represent wind reworking (e.g. Smith & Katzman, 1991; Douillet *et al.,* 2018).

Dimensions

Although referred to as dune-bedforms, pyroclastic DBs range from ripple-sized (backset stratasets of a few centimetres length and thickness) up to over two orders of magnitude greater (*ca* 30 m length, *ca* 3 m thickness; Fig. 4). They are thus much smaller than most aeolian or submarine dunes, and rather correspond to the size of 'megaripples' (as termed in Self & Sparks, 1978). A swarm of datapoints of thickness/lengths (sometimes reported as wavelength and amplitude) is built from deposits of several eruptions, with emergence of a vague linear increase, roughly contained within a ratio of one-third to one-thirtieth (Fig. 4; note that the methods of measurement are not standardized – from a surface bedform or lamination patterns). Exceptionally large dimensions have been reported, yet the associated structures might be related to the stratigraphic backstepping of depositional profiles (length of 60 m in Self & Wright, 1983; 100 m in Sigurdsson *et al.,* 1987; 200 m in Brand & Clarke, 2009 and Brand & Heiken, 2009; 100 to 250 m in Marshall *et al.,* 2015; 520 m long in Brown & Branney, 2004). Spatially, the size of DBs is found to decrease downstream within a deposition zone (see *Main types of patterns* section). Greater dimensions are largely interpreted as reflecting higher flow velocities or 'energy' (e.g. Druitt, 1992; Brand & Clarke, 2012), yet there may also be a fundamental influence of sedimentation rate (or Rouse number) as well as event duration (Table 1, e.g. Valentine, 1987; Douillet *et al.,* 2013a). Interestingly, identical structural patterns can be observed with length scales ranging over two orders of magnitude (for example, Fig. 8A versus 8E, Fig. 6B versus 10C).

Dip angle of lamination

Pyroclastic DBs exhibit an extreme variety of dip angles, regarding both truncations and laminations (e.g. Schmincke *et al.,* 1973; Douillet *et al.,* 2019), and have the specificity to have their stoss generally steeper than their lee (e.g. Moore, 1967; Belousov & Belousova, 2001; Douillet *et al.,* 2013b).

Relatively small structures (<1 m length) are commonly flatter than larger ones, with dip angles on stoss and lee sides generally below 20°. Internally, they comprise subplanar foreset to low-angle backset lensoidal layers, or

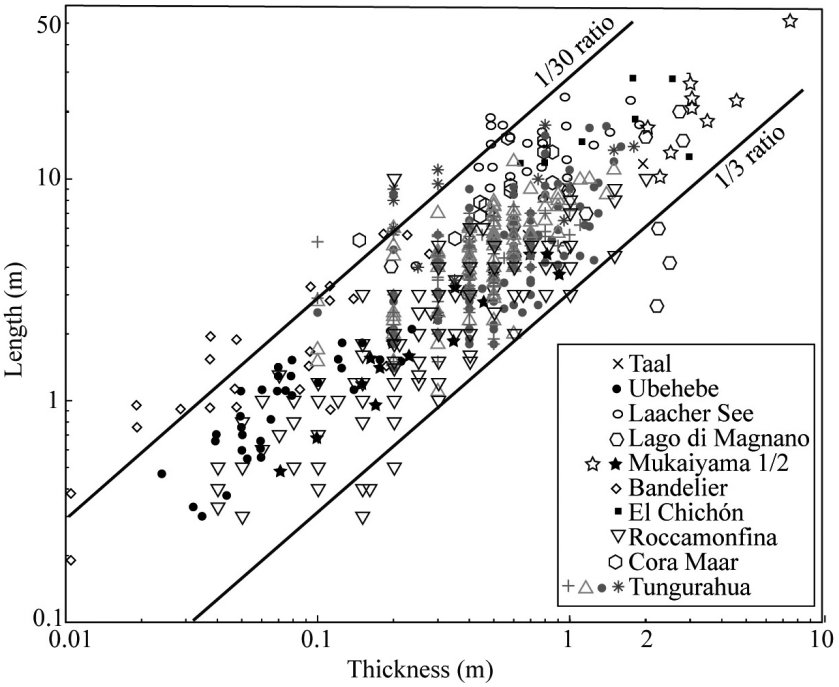

Fig. 4. Dimensions of pyroclastic dune-bedform structures, length versus thickness in logscale. Data compilation from Taal Volcano (Waters & Fisher, 1971), Laacher See (Schmincke *et al.,* 1973), Taal Volcano and Ubehebe Craters (Crowe & Fisher, 1973), Bolsena Caldera, Vico Caldera, Baccano Crater, and Martignano Crater – all four grouped under Lago di Magnano (Mattson & Alvarez, 1973), Mukaiyama (Yokoyama & Tokunaga, 1978; Tokunaga & Yokoyama, 1979), Bandelier Tuff and El Chichón (Sigurdsson *et al.,*1987), Roccamonfina (Gianneti & Luongo, 1994), Cora Maar (Gençalioğlu-Kuşcu *et al.,*2007), and Tungurahua Volcano (Douillet *et al.,* 2013b). Additional available data from Cape Wanbrow (Moorhouse & White, 2016) are not considered adequate here.

aggrading structures resembling hummocky-cross-stratifications (HCS). Low-angle DBs are dominant in deposits from monogenetic, phreatomagmatic eruptions, but occur from any eruption style (for example, at Ubehebe crater: maximum of 23° on stoss and 12° on lee, reported by Crowe & Fisher, 1973).

Steep-sided structures span the entire dimensional range (from centimetric to metric scales). Whereas lee side laminae rarely exceed 20° to 30° dip angles, the steepness is systematically better expressed on stoss sides, which are commonly reworked by steep truncations, up to vertical cuts. The covering truncation-based backset beds mimic the underlying morphology, reaching surprising dip angles up to the vertical on bedsets up to tens of centimetres in thickness (70° reported by Schmincke *et al.,* 1973; 60° by Giannetti & Luongo, 1994; 68° by Brand *et al.,* 2016; 90° by Douillet *et al.,* 2019). Notably, when very steep structures are present, they coexist with low-angle structures. In that case, the structures drastically evolve from subhorizontal to near-vertical during growth, until truncations and aggradation sometimes lead back to a subsequent low-angle configuration. At Tungurahua, where dip angles could be measured on >300 pristine surficial bedforms, angles were reported from 0° to 35° for both stoss and lee faces, with average slopes of 10° to 15° (Douillet *et al.,* 2013b). Thus the surface expressions of bed configurations at the end of an event are much smoother than the internal patterns preserved during the flow.

Main types of patterns

End-member types of pyroclastic DB structures have been variously drawn for specific eruptions, either regarding their internal lamination patterns (five types in Schmincke *et al.,* 1973; three types in Tokunaga & Yokoyama, 1979; five other types in Cole, 1991; eight groups in Wohletz & Sheridan, 1979) or including surficial shapes (four other groups in Douillet *et al.,* 2013b). Based on the literature and numerous observations, four main types of patterns are recognized here (Fig. 2):

Type A (Figs 2A and 5): Subplanar to backset or foreset lensoidal patterns: These are characterized by relative flatness (e.g. type 5 in Schmincke *et al.,* 1973; Colella & Hiscott, 1997; Cole *et al.,* 2001; or 'elongate' in Douillet *et al.,* 2013b). Such patterns occur either isolated growing from flat beds, or forming the base of a subsequently steepening structure or, conversely, towards the top of a structure, when the patterns flatten again.

Type B (Figs 2B, 6, 10 and 11A): Fully climbing patterns (e.g. types b and c in Cole, 1991; 'indulation bedform' in Valentine *et al.,* 1989):

Such laminations are not truncative, relatively steep (20 to 35°), with preservation of the palaeo-crest in laminae, often even with depositional stoss side laminae highlighting formsets. The term 'symmetrical dunes', widespread in pyroclastic literature, yet of unclear meaning, might correspond to patterns of type B as defined here.

Type C (Figs 2C, 7 and 11A): Draped truncations (e.g. types 3 and 4 in Schmincke *et al.,* 1973; Sheridan & Updike, 1975; 'antidunes' in Wohletz & Sheridan, 1979; type a in Cole, 1991; Tokunaga & Yokoyama, 1979): they are characterized by gently truncated stoss covered with massive layers to continuous drapes. Type C makes a continuum with transition to type D.

Type D (Figs 1A, 2D and 8): Steep truncations covered with steep backset strata (e.g. types 1 and 2 in Schmincke *et al.,* 1973; types d and e in Cole, 1991; Tokunaga & Yokoyama, 1979; Brand *et al.,* 2016). Often occurring in upcurrent propagating series (retrogression), where the backset beds against a previous truncation are partially cut by a subsequent truncations more upstream. Eventually, backset bedsets fill up the troughs and flatten the bedform.

These categories represent end-members, and many structures straddle between two of the described types (e.g. Fig. 5B versus 6, Fig. 5 versus 7A to C, Fig. 7D and E versus 8). Notably, all of these patterns can co-exist in a single bedform, either distributed over its vertical extent or evolving laterally (e.g. Figs 7A, 7B and 11A, see lateral evolutions in Douillet *et al.,* 2019). Trough cross-beds and tabular beds are notably rare, yet not totally absent (e.g. Wohletz & Sheridan, 1979; Sohn & Chough, 1989).

Pattern evolution

Surface geometries

Based on datasets from a number of relatively small historical eruptions, DBs could be documented from surface outcrops and surficial shapes (Figs 1 and 9, eruptions from Bárcena in 1952; Taal in 1966; Mount St. Helens in 1980; El Chichón in 1982; Pinatubo in 1991, Tungurahua in 2006). Pyroclastic DBs generally occur in swarms of tens to hundreds of bedforms in surface outcrops (Figs 1B and 9). For PDCs funnelled within ravines, DBs are best documented as grouped within limited deposition zones (hundreds of metres wide) on overbanks of ravines, due to the overspill of turbulent currents (Douillet *et al.,* 2013a). In unconfined settings, DB deposition zones spread from a distance from the eruptive vent and up to several kilometres downstream. Interestingly, a zone of erosive furrows can precede a DB field, with an abrupt transition from erosive to depositional zones (plate 24 in Richards, 1959; see Fisher, 1977, for discussion). The dimensions of DBs decrease downstream away from the eruptive centre in simple radial fashion, or along individual deposition zones when deposits are funnelled – i.e. not directly with distance from the crater – or in zones of lowered topographic gradients (e.g. Moore, 1967; Sigurdsson *et al.,* 1984; Rowley *et al.,* 1985; Douillet *et al.,* 2013a; Lube *et al.,* 2014). In-train patterns are rare (counterexamples: Sigurdsson *et al.,* 1984; 'two-dimensional DBs' in Douillet *et al.,* 2013b). Groups of DBs can show a spatial organization in terms of external shape types. Hoblitt *et al.* (1981) reported a downstream evolution from irregularly shaped hummocks to transverse DBs at Mount St. Helens. At Tungurahua, the shape of DBs evolved from steep 'transverse' shapes in upstream zone of DB fields, with a downstream increase in 'lunate' shapes i.e. crescent pointing upcurrent (Douillet *et al.,* 2013b). On downstream edges of deposition zones and on upslope transport zones, steep and wide (flow-perpendicular) 'two-dimensional' DBs occurred in periodically repetitive bedform trains with short wavelength (Fig. 9; Douillet *et al.,* 2013a, 2013b), an observation corroborated at El Chichón (Sigurdsson *et al.,* 1984). Notably, these spatial trends in bedform shapes follow a pattern observed in analogue flume experiments with supercritical density currents by Spinewine *et al.* (2009). Sigurdsson *et al.* (1987) noted a superimposition of 'larger elongate transverse bedforms up to 100 m in length and smaller (metre-scale DBs) with short and curved crests' in the 1982 El Chichón deposits, similar to the superimposition of short-period 'chutes-and-pools' and long period 'cyclic steps' in analogue flume experiments by Cartigny *et al.* (2014).

Stratification patterns

Studies of internal cross-stratification patterns in the absence of pristine surficial exposures complement the observations on downflow evolution of bedform morphology. Chough & Sohn (1990) suggest a facies evolution with proximal massive deposits, medial planar to dune-bedded deposits, and distal planar laminations (see also Colella & Hiscott, 1997), whereas Wohletz &

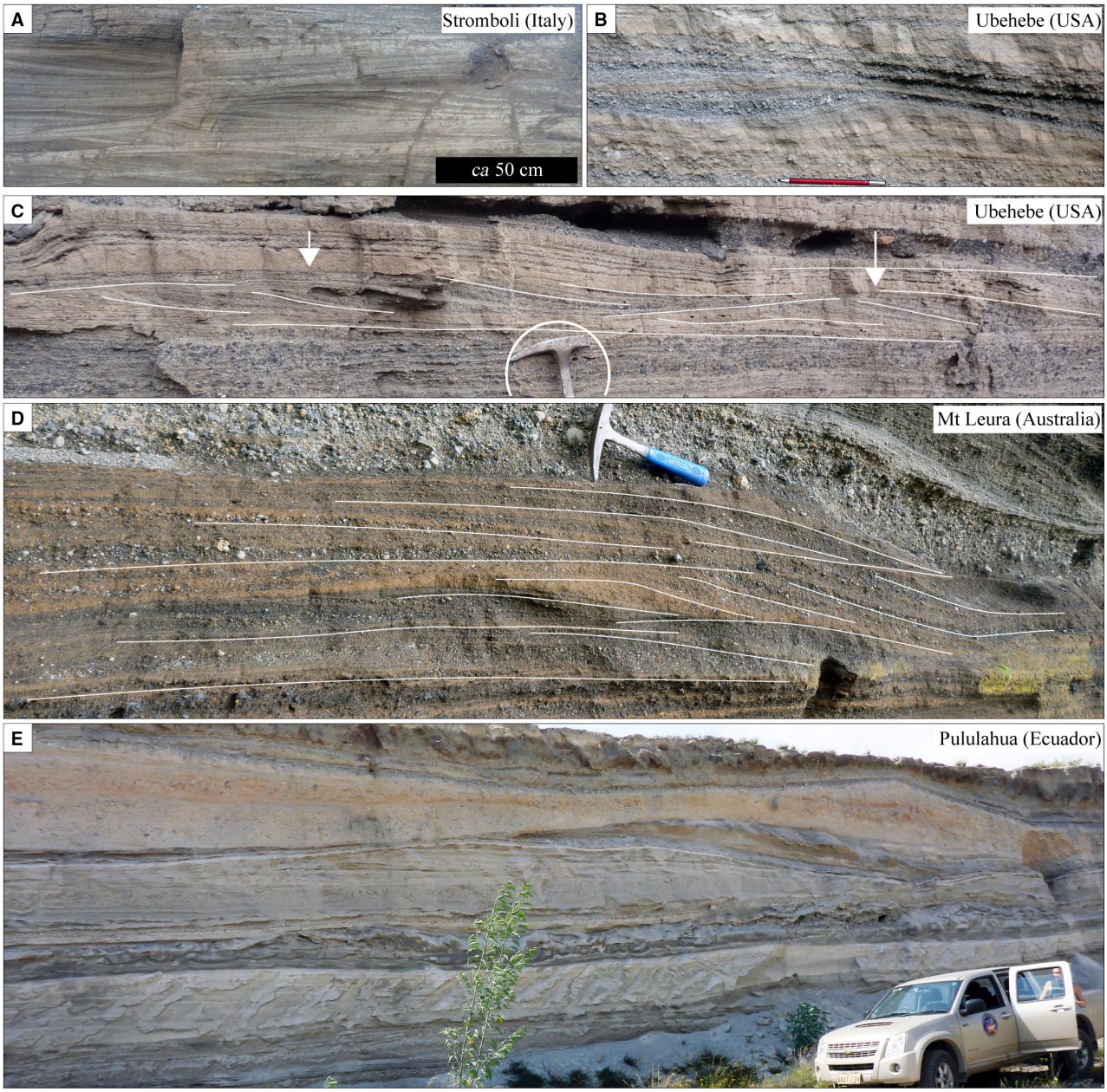

Fig. 5. Low-angle dune-bedform structures (TYPE A). (A) Stromboli, crater area, possibly related to the Holocene 'Secche di Lazzaro succession' (see Giordano *et al.,* 2008); (B) and (C) Ubehebe Crater (see Crowe & Fisher, 1973; Fierstein & Hildreth, 2017). The structure in (B) is low-angle and fully-aggrading (i.e. mixed type A/B), pencil for scale is *ca* 15 cm. A train of two DBs is visible in (C) and transitional to draped truncation type (mixed type A/C), hammer head for scale is 15.5 cm wide. (D) Mount Leura (see Joyce, 2004; Cas *et al.,* 2017), stack of low-angle bedsets, hammer for scale is 28.5 cm long. (E) Large-scale, composite low-angle structure at Pululahua Volcano (see Papale & Rosi, 1993). For all images, flow orientation roughly from left to right; photographs (B), (C) and (D) have been mirrored for consistency.

Sheridan (1979) envision a downcurrent evolution from cross-bedded to massive to planar beds. A general downflow decrease in dimensions has been noted by several authors (e.g. Tokunaga & Yokoyama, 1979; Wohletz & Sheridan, 1979; Cagnoli & Ulrych, 2001).

In terms of type, Schmincke *et al.* (1973) suggested that DB structures of types C and D

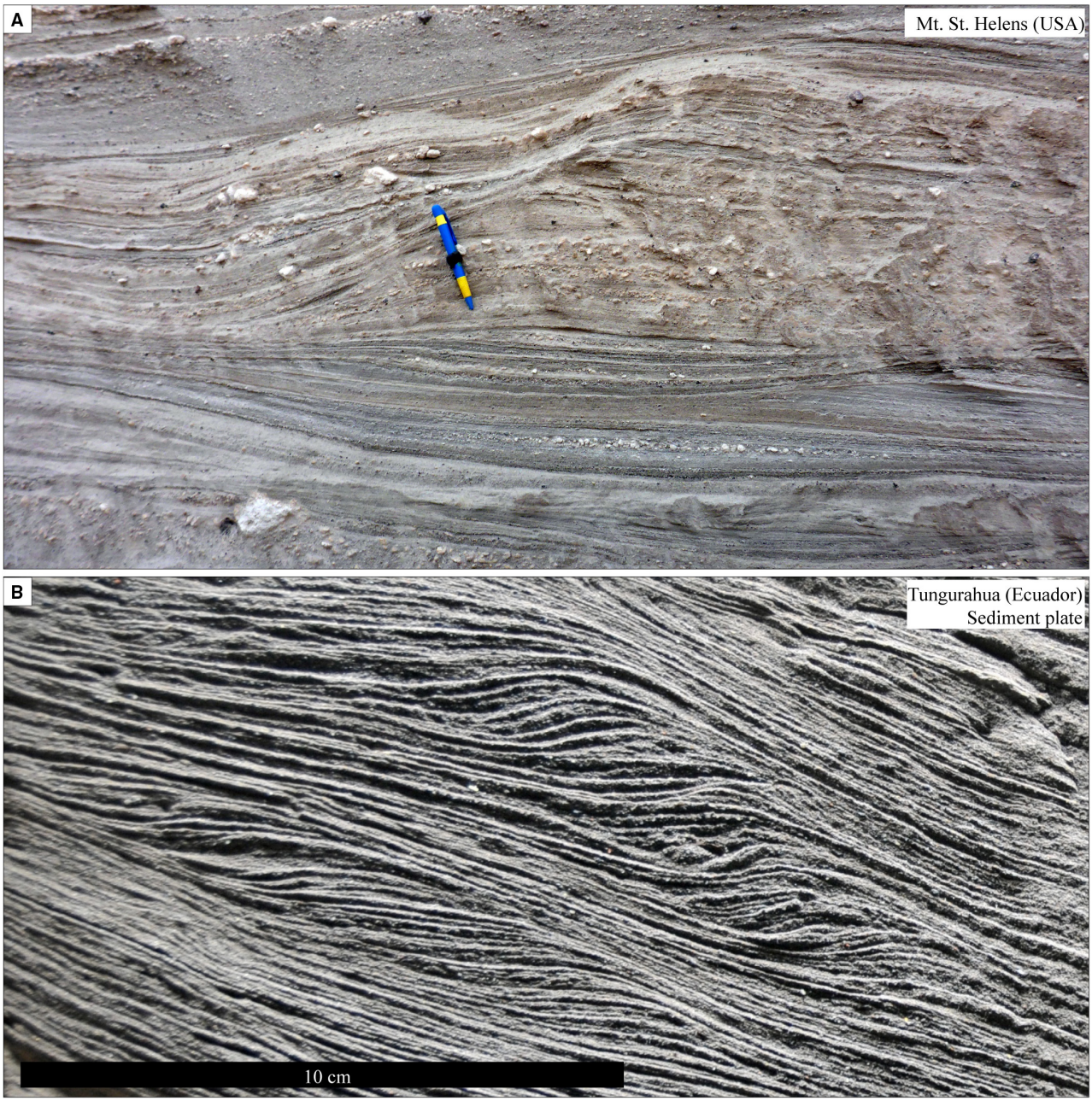

Fig. 6. Fully-aggrading dune-bedform structures (TYPE B). (A) Mount St. Helens (see Rowley *et al.,* 1985; Brand *et al.,* 2016), low-angle to regressive to progressive trend. Pen for scale is 14 cm long. (B) Tungurahua, backset ripples in sediment plates/lacquer peels (see Douillet *et al.,* 2018, 2019). For all images, flow orientation roughly from left to right; photograph (A) has been mirrored for consistency.

would occur in more proximal zones than those of types A and B. At Mount St. Helens, Druitt (1992) observed that the aggradation of DBs formed preferential foreset stratasets where currents passed on the upstream face of ridges, whereas low-amplitude backset or foreset stratasets could develop on the downstream side of hills. For the same deposit, Fisher (1990) observed that crests aggrading uphill and up-current are primarily found on lee side slopes >20°, whereas down-current migration would occur on flat zones. These latter observations contrast with recent field data proving the coexistence of any pattern within a single DB

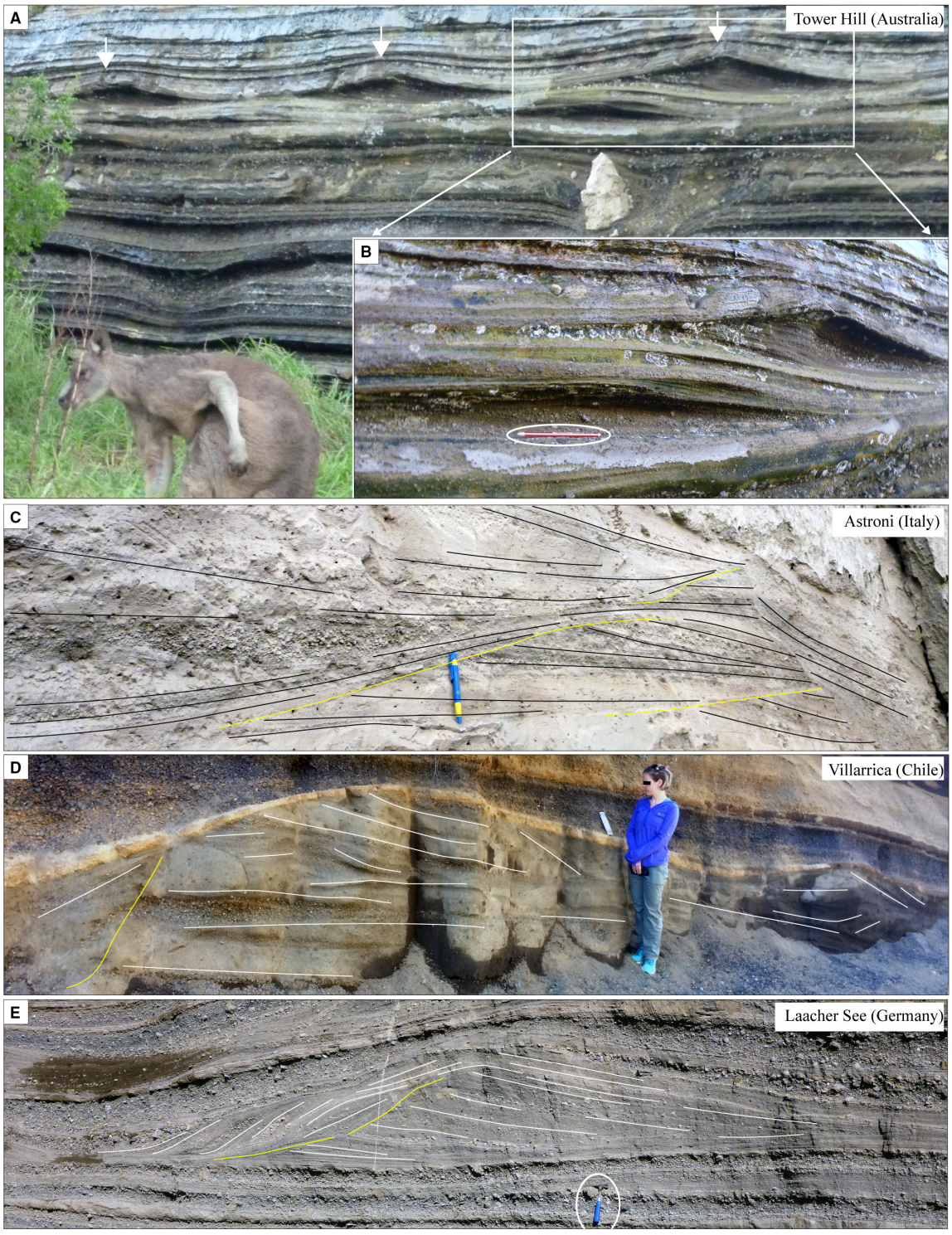

Fig. 7. Truncated dune-bedform structures with overlying beds (TYPE C). (A) and (B) Tower Hill (see Sherwood *et al.,* 2004; Prata, 2012), train of three structures in (A), with zoom in (B) showing transition from low-angle to truncated DB, kangaroo and 15 cm-long pencil for scale (mixed type A/B). (C) Astroni eruption, Campi Flegrei (see Dellino *et al.,* 2004), relatively low-angle and truncated beds, pen for scale is 14 cm long. (D) Villarica, likely 'P2C member' (see Parejas *et al.,* 2010), truncated structure draped by fallout and subsequent flow deposits. Person for scale is *ca* 1.55 m tall. (E) Laacher See (see Schmincke *et al.,* 1973), truncated structure transitional to type D (mixed type C/D), hammer for scale is 28.5 cm long. For all images, flow orientation roughly from left to right; photographs (A), (B) and (E) have been mirrored for consistency.

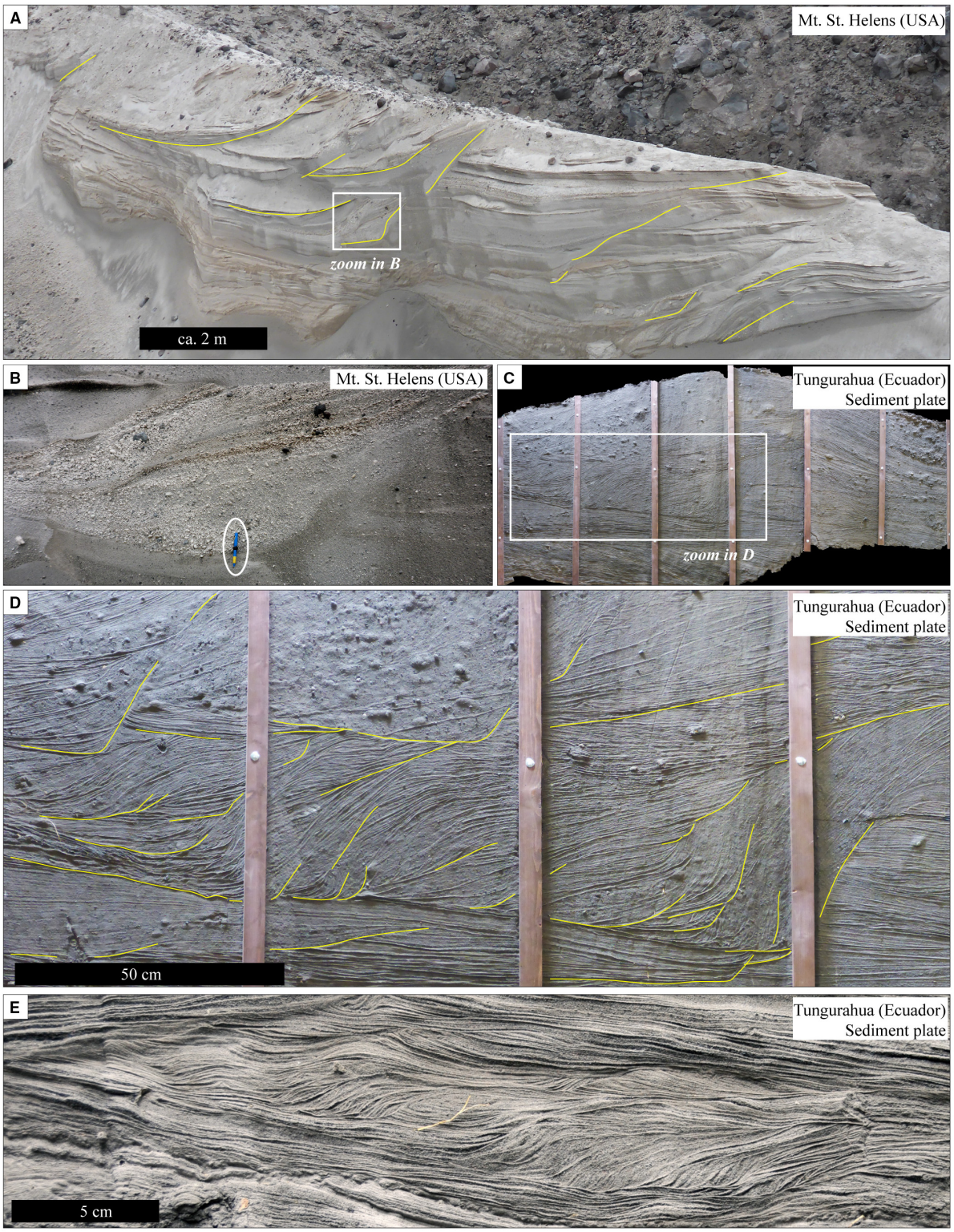

Fig. 8. Trains of backstepping, steep-truncation trains (highlighted) covered with backset beds at various scales (TYPE D). (A) and (B) Mount St. Helens (tens of metres-scale; see Rowley *et al.,* 1985; Brand *et al.,* 2016), zoom in (B) into coarse-enriched backset beds. (C), (D) and (E) Tungurahua (see Douillet *et al.,* 2013b, 2019). Complete dune-bedform in (C) with zoom into truncation trains in (D). (E) Same structure at centimetre-scale and silt-size material, visible only after epoxy impregnation in sediment plates (Douillet *et al.,* 2018). For all images, flow orientation roughly from left to right. Photographs (A) and (B) have been mirrored for consistency.

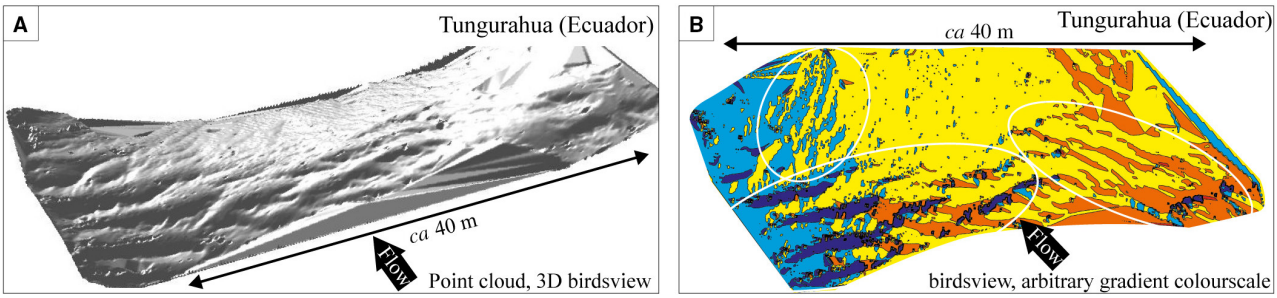

Fig. 9. Repetitive in-train patterns in 'two-dimensional' bedforms at Tungurahua (see Douillet *et al.,* 2013a). Topography point cloud from Terrestrial Laser Scanner data. (A) Three-dimensional bird's-eye view and (B) bird's-eye view of slope gradient, colour scale corresponds to an arbitrary gradient scale. Note trains visible as successive dark blue lines in lower left, successive yellow-orange alternations in lower right, and yellow-blue-sky in upper left.

structure in between parallel cuts separated by tens of centimetres (Douillet *et al.,* 2019). Within a single structure, several types of patterns can coexist (types B, C and D), as well as fractions with dominance of foreset versus backset laminasets, suggesting that the observations of Schmincke *et al.* (1973) and Druitt (1992) may reflect a tendency only, or that they may simply be coincidental. An organization in repetitive periodic trains of two to five DB structures may occur for low-angle DBs (type A, for example Figs 5C and 7A), steep truncations (for example, Fig. 8A, D and E), or fully-aggrading patterns (for example, Fig. 10; e.g. Cagnoli & Ulrych, 2001; Douillet *et al.,* 2019). Where several cross-stratified beds are superimposed, DBs have a strong tendency to build up over the shape of former structures, resulting in vertically stacked DBs at a fixed location, thus forming composite structures (Fig. 11; e.g. 'perched dunes' in Giannetti & Luongo, 1994; Sigurdsson *et al.,* 1987; Douillet *et al.,* 2013b).

Grain-size distributions

Pyroclastic DB structures have grain-size distributions characterized by poorer sorting and spanning a wider range of particle sizes compared to most aeolian and waterlaid bedforms, ranging from silt to gravel sizes (for example, Fig. 8B versus 8E versus 12, Walker, 1984; Love *et al.,* 2018). Within pyroclastic deposits, dune-bedded material tends to overlap in terms of sorting versus mean particle diameter on the finer and better sorted fields of 'granular flows' and 'fallout' end-members (Walker, 1971; Crowe & Fisher, 1973; Sparks, 1976; Walker, 1984). Accretionary pellets are common in DB deposits (e.g. Schumacher & Schmincke, 1991; Dellino *et al.,* 2004). Polymodal distributions are common and deconvolution of signal could help with unravelling superimposed transport mechanisms (e.g. Wohletz *et al.,* 1989; Gençalioğlu-Kuşcu *et al.,* 2007; Douillet *et al.,* 2013a; Mackaman-Lofland *et al.,* 2014; Love *et al.,* 2018). In wind-tunnel experiments with pure winds, the surface roughness and saltation threshold for pyroclasts were found to be roughly similar to those of particles of similar density, providing an estimate for transport and depositional flow velocities (Douillet *et al.,* 2014). The Sauter mean diameter, defining a characteristic length scale for fluid–particle interactions, may represent the most relevant parameter for PDC transport and deposition (e.g. Breard *et al.,* 2019).

Interestingly, the smallest documented pyroclastic structures (few centimetres length) can consist of fine silts, a characteristic absent from larger DB structures (tens of metres length), which are commonly dominated by lapilli/pebble sizes. However, many examples show that grain size is not smoothly distributed with dimensions of DBs (for example, Figs 5D, 6B and 7C), but rather depends on the source material (eruption style). Many DB structures of any type have stoss face backset strification or lenses visually fairly enriched in coarse fractions, but depleted in fines (for example, Figs 5B, 6B, 7C and 8B). In samples from DB structures of type B at Tungurahua, stoss side bedsets were on average better sorted and coarser-grained than lee side ones (Douillet *et al.,* 2013b).

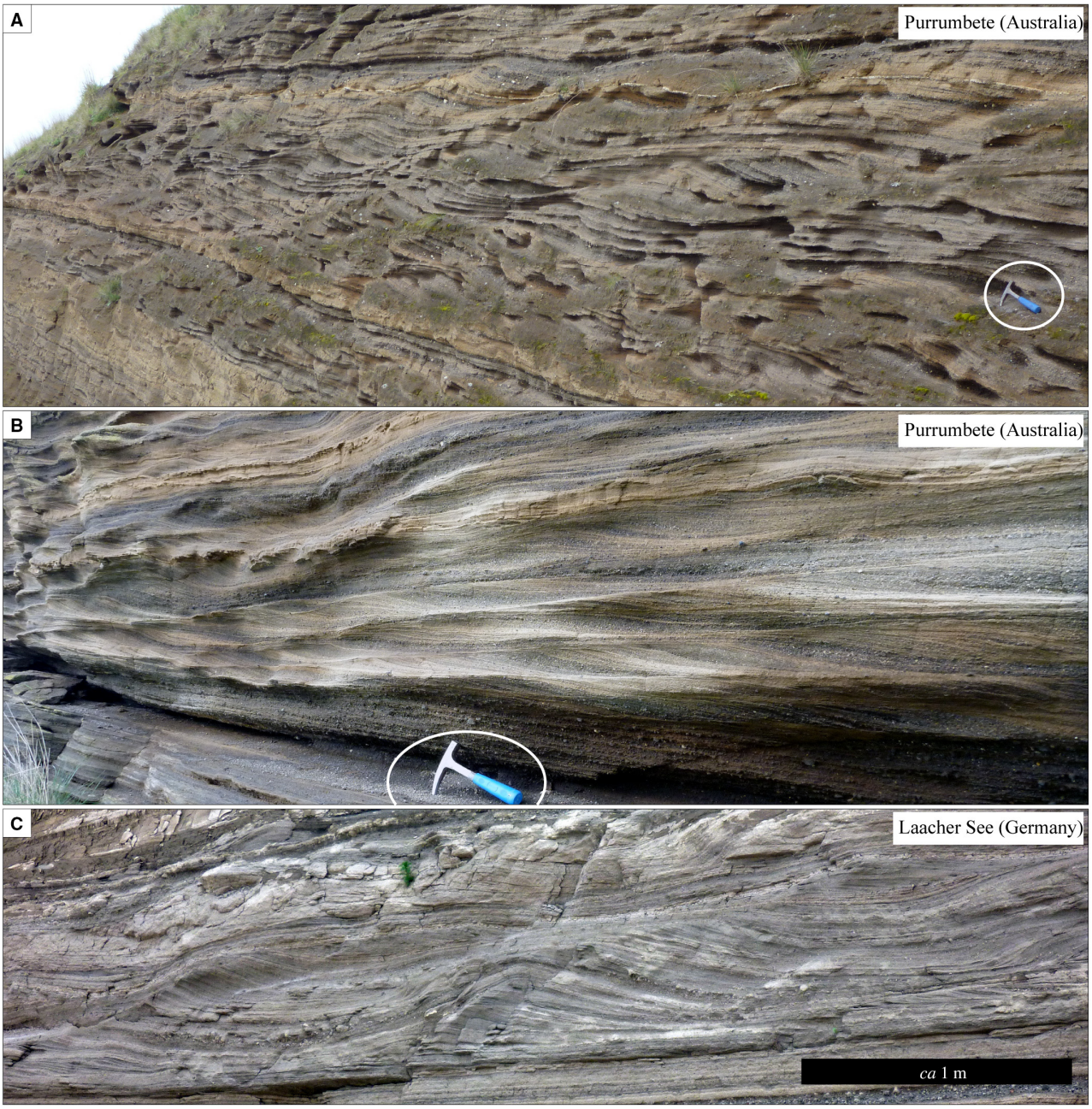

Fig. 10. Periodic trains of aggrading patterns. (A) and (B) Purrumbete (see Jordan *et al.,* 2013). Fully-aggrading patterns in (A), and migrating and climbing patterns in (B), hammer for scale is 28.5 cm long. (C) Fully-aggrading patterns at Laacher See. For all images, flow orientations roughly from left to right; photograph (A) has been mirrored for consistency.

EXISTING INTERPRETATIONS

Seminal work and early interpretations as supercritical bedforms

Pyroclastic DB cross-stratifications were recognized as primary features after the observation of undulating bedforms in deposits of artificial explosions (for example, Bikini 1946 and Sedan 1962 nuclear 'test' bombs; Carlson & Roberts, 1963), or mantling the surface of pyroclastic deposits from historic eruptions (plate 24 in Richards, 1959; Moore *et al.,* 1966; Moore, 1967). From the 1966 eruption at Taal Volcano

(Philippines), Moore described cross-stratification with both stoss and lee side laminae, episodic scouring of the stoss side, steeper stoss than lee angle, and evidence for a slight downcurrent migration of the bedform crests. Cross-strata in ancient successions have initially been termed antidunes as a descriptive term for "low-amplitude bed waves with stoss- and leeside slopes inclined at angles less than the angle of repose" (Fig. 5B and C; Fisher & Waters, 1969). Similarly, Fisher & Waters (1970) 'referred' to PDC DBs as antidunes because of their typical low-angle lamination contrasting with the steeper lee side dip angles (at or near the angle of repose) of subcritical bedform laminae evidenced by Simons & Richardson (1966).

Waters & Fisher (1971) were the first to use antidune in its hydrodynamical meaning, i.e. as an interpretative term for structures formed under a standing wave at a relatively sharp density interface between the moving bed load and the overriding PDC cloud. Their argument was that the shape and internal cross-stratifications resembled antidunes produced in flume experiments by Middleton (1965), and described from turbidite outcrops interpreted as antidunes by Walker (1967). Waters & Fisher (1971) noted that only a high depositional rate would permit preservation of antidune cross-stratifications, likely to occur in PDCs. Crowe & Fisher (1973), re-using the illustration of Fisher & Waters (1969) and Mattson & Alvarez (1973), followed the antidune interpretation of Waters & Fisher (1971) for several other volcanoes, applying equations for stationary surface-gravity waves and supercritical flows for palaeohydraulic calculations.

Schmincke *et al.* (1973) observed decametre scale structures with backset and foreset stratification (fully-aggrading) and instances of preserved upstream migration of the crest (regressive), but with steep stoss and lee sides (Figs 7E, 10C and 11A). Even if the primary evidence of Fisher & Waters (1970) for facies interpretation was not observed (i.e. stoss and lee sides below the repose angle), Schmincke *et al.* (1973) interpreted these structures as the products of antidunes. These authors thoroughly focused on structures made from stoss-aggrading lensoidal layers deposited in front of steep erosive surfaces that they attributed to more proximal areas. As such, these structures were regarded as representing higher-energy bedforms than antidunes, and thus interpreted as 'chutes-and-pools' (Figs 11A and 12B).

Followers and detractors of the supercritical interpretation

With a few exceptions, most authors have followed the pioneering work and used 'antidune' and 'chute-and-pool' either as a descriptive and/or interpretative term, without further discussion of the question. The terms were sometimes adopted for a combination of descriptive and interpretative purposes (and jump between one or the other), shortcutting any further discussion. There has been a pervasive tendency to call 'subcritical' any sedimentary structures with foreset beds only, and 'supercritical' any structures including backset stratification (Mattson & Alvarez, 1973; Fisher, 1977; Waitt *et al.,* 1981; Fisher *et al.,* 1983; Self & Wright, 1983; Rowley *et al.,* 1985; Valentine, 1987; Valentine *et al.,* 1989; Giannetti & Luongo, 1994; Bryan *et al.,* 1998; Sohn & Park, 2005; Gençalioğlu-Kuşcu *et al.,* 2007; Kelfoun *et al.,* 2009; Brand & White, 2007; Brand *et al.,* 2009; Brand & Clarke, 2012; Valentine, 2012; Pedrazzi *et al.,* 2013; Marshall *et al.,* 2015; Moorhouse & White, 2016). Additionally, pyroclastic DB stratification has been reported but without being the specific focus of study, lacking a detailed description or not being discussed in terms of formative flow regime (e.g. McDonough *et al.,* 1984; Wilson, 1985; Boudon *et al.,* 1993; Cole *et al.,* 1993, 2001; Scott *et al.,* 1996; Colella & Hiscott, 1997; Bestland & Krull, 1999; Allen, 2001; Cagnoli & Ulrych, 2001; Németh *et al.,* 2001; Dellino *et al.,* 2004; Brown *et al.,* 2007, 2008; Sulpizio *et al.,* 2007; Parejas *et al.,* 2010; Mattsson & Tripoli, 2011; Cas *et al.,* 2017). An in-depth consideration is often hampered by unclear nomenclatures mixing description and interpretation, as well as by confusions on flow-dynamics concepts. The initial arguments of early authors were lost, i.e. that antidune structures were characterized by low-angle lamination, and that steep backset bedsets formed in the subcritical part of a chute-and-pool configuration (Waters & Fisher, 1971; Schmincke *et al.,* 1973). Consequently, any sedimentary structure with more or less draping beds was seen as the product of antidunes, and any stoss-erosive one as the product of chutes-and-pools.

The first detractor of the supercritical interpretation was Allen (1984), who considered it 'bolder' in his general sedimentology textbook. Allen (1984) suggested that upstream aggradation and migration was a plastering effect due to

Fig. 11. Stacking of dune-bedform structures at a fixed location. (A) Laacher See (person for scale is *ca* 1.7 m tall) and (B) surface exposure at Tungurahua with multiple stacked crest lines visible (see also Douillet *et al.,* 2013b). For all images, flow orientation roughly from left to right.

the cohesion of particles in the presence of liquid water in PDCs, whereas downstream migrating bedforms would be limited to 'dry surges' (see also Carey, 1991). This process model was disproved by two in-depth studies by Cole (1991) and Druitt (1992), which showed that both upstream and downstream-accreting bedforms could occur during the same eruptive event. Hence, aggradation patterns were not related to water content, but to local changes in the flow characteristics. The dimensions of DB structures produced in wet versus dry eruptions are similar (Fig. 4), accretionary pellets may occur in both, and no distinctive characteristics in stratification patterns were identified in this review.

Alternatively, it has been suggested that backset stratasets may actually represent foresets deposited under reversed flows. Fisher (1990) suggested a decoupling of the transport and depositional system, so that secondary basal granular flows could flow downslope against the direction of the main current (locally travelling upslope), to form the final structures. Andrews & Manga (2012) proposed that the uplift of a phoenix cloud in the proximal part

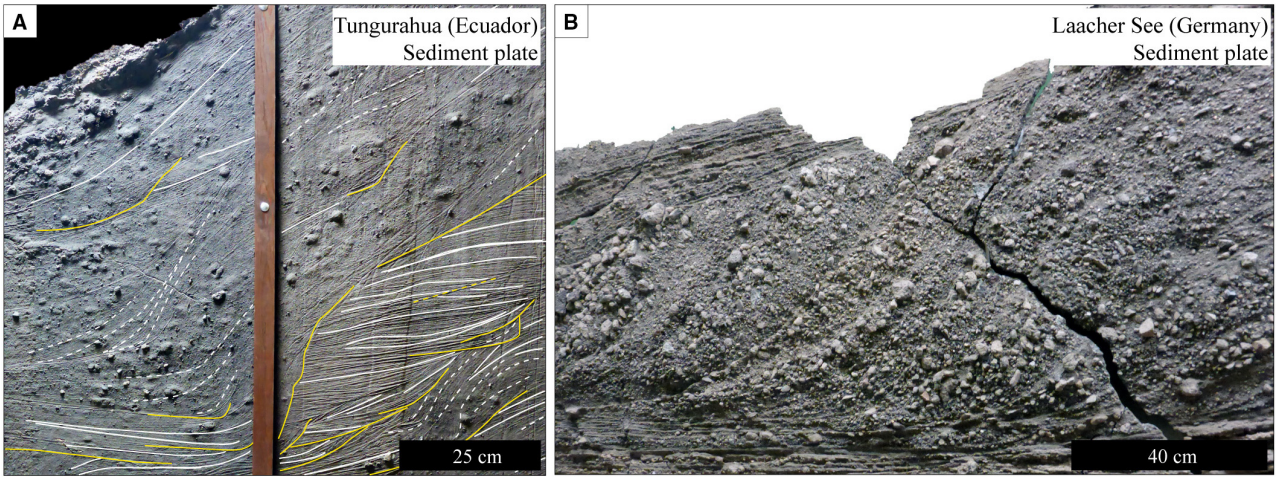

Fig. 12. Backset beds enriched in coarse fraction with 'lineation patterns' rather than well-defined stratification represent possible examples of deposits from granular Froude jumps. (A) Tungurahua and (B) Laacher See. Lineations are only visible after impregnating the outcrop with epoxy resin to produce sediment plates (Douillet *et al.,* 2018). For all images, flow orientation roughly from left to right.

of a flow could suck back a PDC front, thus creating a local flow reversal that might have a sediment signature with apparently regressive DBs. Although such reversed-flow processes may occur in particular cases, there is various evidence that most pyroclastic DBs are purely primary features related to a relatively consistent flow direction, based on the orientation of clast imbrications, truncations and sheared structures (e.g. Schmincke *et al.,* 1973; Douillet *et al.,* 2013a, 2015, 2018). Still, using reasonable flow relations in an antidune equation framework, most pyroclastic bedforms appear too steep to support a supercritical-flow origin (Charland & Lajoie, 1989; Douillet *et al.,* 2013b).

Some authors have discussed and interpreted pyroclastic DB structures as lower-regime bedforms (e.g. Boudon & Lajoie, 1989; Charland & Lajoie, 1989; Sohn & Chough, 1989; Chough & Sohn, 1990), or cautiously used a nomenclature mentioning 'climbing dunes' exclusively (e.g. Self & Sparks, 1978; Cagnoli & Ulrych, 2001; Cole *et al.,* 2002).

PLAUSIBLE INTERPRETATIONS

Stoss-aggradation unrelated to supercritical conditions

A pervasive belief in pyroclastic literature is that foreset bedding would be diagnostic for subcritical-flow conditions at time of deposition, and backset for supercritical conditions. A field study of parallel cuts within a single pyroclastic DB has recently demonstrated the co-existence of steep erosive-based backset laminasets (type D), fully-aggrading stoss-aggrading laminasets (type B) together with stoss-eroded lee bedsets within the same structure (Douillet *et al.,* 2018, 2019). The crude shortcut of a simplistic interpretation based purely on the dip of stratasets is thus not applicable, since it would imply the unlikely synchronous co-existence of a chute-and-pool, antidune and subcritical dune bedform in a single sedimentary structure.

Foreset strata are neither uncommon in supercritical-flow structures, nor diagnostic for subcritical conditions. Stoss-eroded foreset beds may well represent remnants of a formerly fully-aggrading, progressive or regressive structure. It has been demonstrated in analogue experiments and highlighted in several studies that supercritical conditions may lead to foreset stratification and downstream migrating structures (e.g. Carling & Shvidchenko, 2002; Spinewine *et al.,* 2009; Ito, 2010).

It is here considered that backset bedding should not necessarily be ascribed to supercritical conditions and can occur in a variety of settings. Sigurdsson *et al.* (1987) related the formation of pyroclastic DBs to a combined effect of saltation-bedload transport, together with a suspension component (see also Cole & Scarpati, 1993, and the 'simultaneous fallout

and surge' in Valentine & Giannetti, 1995). Building on this idea, a mechanism of 'differential-draping' was suggested for fully-aggrading structures with continuous stoss to lee side laminae, including preferential upstream aggradation (Douillet *et al.,* 2013b). 'Differential-draping' is unrelated to supercritical conditions, and would correspond to a fallout-modified process over an inherited topography, affected by a slow-moving current (i.e. below or close to the saltation threshold) and high aggradation rates. Wind-tunnel measurements with pure wind and pyroclasts show that the threshold for saltation can be 50% higher on a 20° upslope incline (stoss side analogue) than on a −25° downslope face (lee side analogue) (Douillet *et al.,* 2014). This result has been suggested to explain preferential aggradation on stoss faces as well as upstream-aggrading bedforms unrelated to antidunes, and is supported by field evidence (see fig. 6C in Douillet *et al.,* 2019).

Antidunes

The argument to interpret certain sedimentary structures as the products of antidunes in the seminal literature was related to the flatness or low relief of bedforms, as observed from open-channel water flows (e.g. Waters & Fisher, 1971; Crowe & Fisher, 1973; Self & Wright, 1983; Druitt, 1992). Rapid and shallow supercritical currents are unlikely to create steep bedforms. Any antidune growing too steep would lead to a chute-and-pool configuration. Taking into account the previous consideration of non-uniqueness of backset/foreset formation, flatness is here considered a necessary argument to infer antidunes in pyroclastic DBs. Thus, only patterns of 'type A' would be eligible for an interpretation as antidunes in pyroclastic DBs (Fig. 5; e.g. Douillet *et al.,* 2013b), in accordance with the initial interpretation (Waters & Fisher, 1971; Crowe & Fisher, 1973).

Steep sided, stoss-aggrading, fully-aggrading DB structures (type B, Fig. 6) are largely taken as antidunes as well in the literature. However, field observations of pyroclastic DB stratification of type B (and C and D) share very few attributes with deposits from most experimental work on antidunes, independent of a deposition rate or environment (e.g. Alexander *et al.,* 2001; Spinewine *et al.,* 2009; Cartigny *et al.,* 2014). Furthermore, the measured dimensions and steepness (>35° slopes) are not compatible with antidunes and are disqualified by a quantitative analysis, since the parent underflows should be less than 15 cm deep with a velocity <1 m s^{-1} (Charland & Lajoie, 1989; Douillet *et al.,* 2013b). Additionally, the uncommon occurrence of series of periodic, in train patterns, and the important spatial stability of pyroclastic DBs are contrasting with the dynamics of free-surface gravity waves. Further, fully-aggrading DB structures can exhibit preferential downstream or upstream aggradation, yet lee side erosion is virtually absent. Given that an antidune is a morphological bed reflection of a gravity wave (a 'mould'), when backset bedding occurs, it should be associated with concurrent lee side erosion due to the mould being translated upstream (Douillet *et al.,* 2013b, 2019).

Some authors have suggested that DB bedding of type C (i.e. low-angle truncated structures with draping beds, Fig. 7) could represent antidunes (e.g. Schmincke *et al.,* 1973; Wohletz & Sheridan, 1979). Besides the aforementioned arguments, in that case, the associated gravity wave would be moulded by a pre-existing bedform, so that it would be driven by the basal topography rather than by the free-surface. As such, this rules out antidunes in the sense of a a bedform moulded by a free-surface wave. Existing estimations of emplacement velocities using an antidune equation framework for pyroclastic bedforms >100 m length are extremely high (52 to 73 m s^{-1}, Brand & Clarke, 2012). Whereas such high velocities may occur during transport (e.g. Scolamacchia & Schouwenaars, 2009), they might be too high to lead to deposition, since they are far above the threshold for saltation for pyroclasts (6 to 8 m s^{-1} near-bed velocities e.g. Douillet *et al.,* 2014, 2019).

The subcritical zone of a Froude jump/erosive chute and depositional pool

Even if DB structures of type B, C and D seem unrelated to antidunes and direct supercritical conditions, one can envisage the formative process to be related to the pool of a Froude jump. Pyroclastic DB stratification of type D has been interpreted as the product of chutes-and-pools since the seminal manuscript of Schmincke *et al.* (1973). Indeed, the typical pyroclastic DB patterns, with alternation of purely depositional phases with stoss face scouring and subsequent infill with coarse-grained backset bedding, share similarities with experimental deposits and some coarse-grained sedimentary structures interpreted as formed by chutes-and-pools in

deposits of other environments (e.g. Postma *et al.,* 2014; Massari, 2017; Lang *et al.,* 2021). This interpretation is strengthened by the common fines-depletion and coarse-enrichment within the toe of backset beds, suggesting an increased turbulence and loss of capacity, coherent with a Froude jump or a basal-blocking process (Figs 8B and 12, e.g. Schmincke *et al.,* 1973; Cole & Scarpati, 1993; Douillet *et al.,* 2019). Additionally, truncation surfaces may become almost vertical and show overturned laminae at the truncation front (type D, Fig. 8). This latter result was reproduced experimentally by eroding a bedform with a short-lived air burst used to mimic turbulent pulses, yet it may be related to the oscillation of the shooting part of a Froude jump as well (Douillet *et al.,* 2017). A similar signature with truncations underlined by overturned laminae has been observed in experimental Froude jumps, and may develop from natural density currents (Postma *et al.,* 2014).

For a chute-and-pool interpretation to be realistic, a shooting (supercritical) flow should impact the stoss of a bedform, erode it, and a Froude jump would have to retreat rapidly upstream, allowing the formation of backset beds. In this frame, the backsetting would be the signature of deposition in the subcritical pool, and not related to supercritical conditions, the latter being limited to the erosion phase. Steep erosive fronts can occur in a series of several truncations cutting one another and stacking in an upstream direction (Fig. 8). Again, this is compatible with an upstream-retreating Froude jump, yet it could also result from internal short-lived bursts or pulses related to turbulence or coherent flow structures near the bed. In such a scenario, the Froude jump would rather be a consequence of a bed topography than occur spontaneously; however, necessary process evidence is still lacking for further discussion.

Additional to type D, it is here considered that patterns of type B and C could well represent the signatures of chutes-and-pools as well. Type C may be envisioned as a transitional form to D, having only lower-angle truncation, and as transitional form to type B, sharing the same internal organization apart from the occurrence of a truncated stoss side. Central in this interpretation is that patterns of type B, C, and D coexist laterally within a single DB structure, and during the same time interval. They are thus likely to represent the same phenomenon, yet with more or less competence (i.e. ability to erode) depending on whether the exposure belonged to the centre or side of the DB structure. Indeed, aside from the truncation, the aggrading parts of these structures, often showing preferential stoss side aggradation and steep backset beds, share most of the characteristics of backset beds within type D patterns (Figs 6 and 10). A sudden drop in competence of the currents, as in a Froude jump, may well explain such structures. Further, citing Chough & Sohn (1990), the often encountered 'smooth and rounded crests without brinkpoints suggest that the bedforms did not entail flow separation', a result that could be attributed to the conditions in the 'pool' of a Froude jump. The mechanism of 'differential-draping' suggested for patterns of type B (Douillet *et al.,* 2013b), which corresponds to a fallout process influenced by a slow moving current over an inherited topography, is fully compatible with an occurrence in the subcritical part of a Froude jump. As such, pyroclastic DBs of type B, C, and D would thus all be related to chutes-and-pools, the different types solely being influenced by the advance or retreat of the erosive/depositional front of the Froude jump.

Interestingly, besides the interpretation of DBs, large-scale sediment bodies, being either lithic breccias (e.g. Macıas *et al.,* 1998) or entire deposition zones covered with DBs (Douillet *et al.,* 2013a), have been postulated to result from Froude jumps of the entire flows at break in slopes. As such, these features could represent giant chutes-and-pools.

Possible rare cyclic steps

There has been an enthusiastic emphasis on cyclic steps in recent sediment literature, especially in the context of sedimentation from density currents (Parker *et al.,* 1996; Cartigny *et al.,* 2011; Dietrich *et al.,* 2016; Slootman & Cartigny, 2020). Cyclic steps are trains of generally asymmetrical bedforms separated by stable, migrating Froude jumps, characterized by a transition from transcritical to subcritical flow over their stoss face to supercritical flow over their lee face. Documented cyclic steps are notorious for their periodic in-train repetition and their upstream-directed migration concomitant with prevalent deposition on gently dipping stoss faces and erosion on the lee sides. The growing recognition of cyclic steps formed by subaqueous density currents legitimises the question of their possible identification from pyroclastic deposits. However, most pyroclastic DB structures share

little with those documented from cyclic steps. In particular, lee side erosion is rare, bedforms are fairly irregular, repetitive in-train patterns are uncommon (although not rare), and backset strata are extremely steep. The occurrence of cyclic steps, however, may be hypothesized for several cases.

Sigurdsson *et al.* (1987) noted a superimposition of "larger elongate transverse bedforms up to 100 m in length and smaller [m-scale DBs] with short and curved crests" at the surface of the 1982 El Chichón deposits. This observation fits with the superimposition of short-period 'chutes-and-pools' and long period 'cyclic steps' observed in analogue flume experiments by Cartigny *et al.* (2014), and might represent a rare documented case of cyclic steps in pyroclastic deposits. In such a case, large-scale undulations would represent the preservation of cyclic steps. Another insight could come from surface shapes observed at Tungurahua, where DBs exhibit a downstream transition in shape from straight-crested 'transverse' to crescent shaped 'lunate' morphology, ending with wide, straight-crested 'two-dimensional' bedforms (Fig. 9; Douillet *et al.,* 2013a, 2013b). This spatial morphological succession is strikingly similar to experimental results with subaqueous density currents of supercritical flows interpreted as representing cyclic steps (see figs 17 to 19 in Spinewine *et al.,* 2009). This would imply that all of these DBs could actually represent cyclic steps. Further data is needed to validate hypotheses on the recognition of cyclic steps, in particular regarding the crests' knickpoints, the steepness of bedforms, and the consequent implications for the scale and stability of the parent flows; however, this interpretive possibility remains open.

Another possible occurrence of cyclic steps in pyroclastic DBs is represented by in-train, repetitive patterns of fully climbing structures of type B (Figs 10 and 11). If DB stratification of type B may represent the pool of Froude jumps, as suggested above, then trains of fully-aggrading DB structures may represent small-scale cyclic steps. These structures further represent an uncommon case of stable deposition from periodic bedform trains, and their geometry resembles that of some submarine sediment waves, all of these characteristics being compatible with those of cyclic steps (see e.g. Cartigny *et al.,* 2011; Pope *et al.,* 2018; Slootman & Cartigny, 2020).

Granular bedforms and granular Froude jumps

Granular flows have long been speculated to participate in DB formation. The cross-bedded character of pyroclastic DB structures commonly evolves into a massive facies within a single genetic unit (and vice versa), passing through 'faint stratification' or lineations, suggesting transitions from (and to) granular flows, saltation and fluid-supported suspension (Figs 8 and 12; e.g. Walker *et al.,* 1981; Fisher, 1990; Cole & Scarpati, 1993; Scott *et al.,* 1996; Colella & Hiscott, 1997; Allen & Cas, 1998; Branney & Kokelaar, 2002; Cole *et al.,* 2002; Brown *et al.,* 2007; Brown & Branney, 2013; Douillet *et al.,* 2019). Although a cross-laminated organization is largely interpreted as resulting from tractional transport (e.g. Branney & Kokelaar, 2002), insights are growing that granular-based currents could also form some stratification (Breard *et al.,* 2018; Douillet *et al.,* 2019; Smith *et al.,* 2020). Indeed, stratification deposited from granular flows may result from spontaneous clast segregation (e.g. Makse *et al.,* 1998; Cizeau *et al.,* 1999), or via turbulent-like 'granulence' effects (Radjai & Roux, 2002; Combe *et al.,* 2015). The stepwise aggradation concept considers that each lamina within a strataset is an extremely thin and massive layer individually deposited in an *en masse* manner (e.g. Sulpizio *et al.,* 2007; Doronzo & Dellino, 2014; Smith *et al.,* 2018). It has long been speculated that granular underflows and traction carpets at the basal bed boundary of PDCs participate in the formation of DBs in the form of aligned grain fabrics, lineations and faint-stratification (Schmincke *et al.,* 1973; Sheridan & Updike, 1975; Cole *et al.,* 2002; Love *et al.,* 2018; Douillet *et al.,* 2019; Brosch & Lube, 2020). Fisher (1990) even considered that secondary granular gravity flows may flow against a PDC's general flow direction following the slope gradient, and deposit stratified DB structures.

In this framework, thick, stoss-aggrading, lensoidal backset layers were understood as being formed by the basal blocking of a granular-based PDC in correspondence with bed irregularities (Fig. 12; Freundt & Schmincke, 1985; Douillet *et al.,* 2013b, 2019). Such an interpretation is supported by granular flow experiments and complemented by dynamical observations that show the development of a phenomenon similar to a Froude jump, referred to as a 'granular jump' (e.g. Boudet *et al.,* 2007; Johnson & Gray, 2011; Viroulet *et al.,* 2017; Smith *et al.,* 2020).

Field and experimental evidence concur to suggest that the formation of such bedforms is initiated in the 'subcritical' part of a granular Froude jump triggered by the pre-existing bed topography (Brennen *et al.,* 1983; Freundt & Schmincke, 1985; Douillet *et al.,* 2019; Smith *et al.,* 2020). Pyroclastic DBs could thus contain a rare natural example of bedforms created by Froude jumps occurring in granular flows.

Besides, for many DB structures of type C, a stratified formset structure is overlain by massive deposits infilling and interacting with the bed (e.g. Fisher *et al.,* 1983). These thus represent a form of granular flow interacting with a pre-existing bedform, and participating in its development (see also elongate DBs in Douillet *et al.,* 2013b). Rowley *et al.* (2014) showed experimentally that a succession of stacked surfaces deposited from fluidized flow could result from progradational or retrogradational accretion and result in patterns similar to many natural pyroclastic DB structures. Such patterns could correspond to forms of granular Froude jumps, or even granular antidunes. An interpretation of DBs as products of basal granular flows would imply an extremely short timescale for their growth, in the order of seconds. Further, the basal granular flows would be largely dominant in shaping the bedform; in other words, the thin depositional system would not contain a record of the transport system, and thus of the vast majority of the upper parts of the carrying currents.

QUESTIONS AROUND SUPERCRITICAL INTERPRETATIONS

Internal density stratification and Richardson number

The sedimentary dynamics of a mobile bed in the supercritical regime are understood to be strongly correlated to the upper free surface of the flow dictating the growth of bedforms. The Froude regime being related to a restoring gravity force, this free surface must be a density interface. Further, the metric scale of individual pyroclastic DBs contrasting with the hundreds of metres in thickness of the visible envelope of a PDC, the free surface interacting with the bed during deposition must be an internal interface within the lower part of the current, probably governed by density stratification (e.g. Schmincke *et al.,* 1973; Valentine, 1987). Whether this density interface is a sharp or a smooth gradient is unresolved, yet PDCs are thought to be vertically stratified in density and experiments support the existence of a basal dense region (e.g. Burgisser & Bergantz, 2002; Breard *et al.,* 2016). In an interpretation in terms of antidune, the depth-dependent Brunt-Vaisala frequency (e.g. Vallis, 2006, p. 92) would represent the relevant length scale for an 'internal gravity wave' (e.g. Valentine, 1987; Carey, 1991). The flow depth at which the relevant interface would occur is unclear, but should lie somewhere below the (wave)length of DBs. It has been stressed that such underflows should be very thin (<15 cm) and slow (<1 m s^{-1}) to create metre-scale DBs (Charland & Lajoie, 1989; Douillet *et al.,* 2013b). However, the existence and stability of such an oscillating density interface represented by a slight contrast of particle concentrations seem questionable for PDCs. Would it not be erased by turbulent mixing or temperature buoyancy effects before any undulation interacts with the bed? In other words, the Richardson gradient numbers (ratio of buoyancy over shear/turbulent mixing, Table 1) in a PDC may not allow a stable density interface to develop and create supercritical underflows. Even if these interfaces occur and are stable over the timescale of a bedform's growth (possibly seconds to hours), the presence of the underflow might form a depositional system partly decoupled from the transport system, and thus informing only on basal flow-boundary processes.

Rarity of stable bedforms

In an interpretation of DBs as upper-flow regime bedforms, antidunes would represent only a marginal portion of pyroclastic DB deposits, whereas the vast majority would be related to the pools formed by Froude jumps. Similarly, cyclic steps would only be a rare end-member confined to large structures. A first explanation may be that antidunes and cyclic steps may be essentially erosional and unrecognized, or have very little preservation potential in a PDC environment. Three specific reasons tied to PDCs can be considered to explain the dominance of chutes-and-pools over cyclic steps and antidunes: sedimentation rate, pulsation and unstable interfaces.

1 At high sedimentation rates, the onset of an antidune will be rapid and abruptly destabilize the flow, leading to the growth of Froude jumps

and 'chutes-and-pools'. Thus, if any, signs of antidunes could be preserved as incipient structures (small-scale DB patterns of 'type A'), and they would be directly overrun and possibly reworked by chutes-and-pools. Additionally, the later growth of steep-sided chutes-and-pools may in turn impede any transition to the cyclic-step stability field.

2 Pyroclastic density currents may be far more pulsating, turbulent and short-lived than most natural density currents (e.g. Vazquez & Ort, 2006; Andrews & Manga, 2012; Pedrazzi *et al.,* 2013; Andrews, 2019). As a consequence, it may be impossible to maintain flow conditions for a prolonged enough time within the stability regime for stable trains of antidunes and cyclic steps to grow and be preserved. A minimal timescale might never be reached, apart from rare sustained eruptions with long runout and long duration (longer than the minutes to hours of a typical eruptive pulse).

3 As mentioned above, the stability of a density stratified PDC may be questioned, the growth of a wave interface for antidunes may be impeded by the transient nature of the density contrasts, and only allow for Froude jumps to grow. A detailed physical study of the relevant equation frames would be needed to provide further evaluation on this hypothesis.

Supercritical can be low-energy and waning

Based on grain-size distribution data, Walker (1984) concluded that dune-bedded deposits correspond to 'weak' events, in agreement with measurements of the saltation threshold for typical pyroclastic grains (Douillet *et al.,* 2014) and structural characteristics (Colella & Hiscott, 1997; Douillet *et al.,* 2013b). In parallel, the observation that steep backset beds grow up to the uppermost laminae at the surface of recent pristine deposits, show that these must correspond to the final stage of events (Douillet *et al.,* 2013b, 2019), an observation in agreement with the transition of DB structures into draping patterns (Dellino *et al.,* 2004; commented by Le Roux, 2005). Backset laminasets thus at least partly record waning and/or depleting dynamics, in agreement with low-energy 'weak' events, and highly depositional dynamics has been emphasized by most authors.

Although supercritical flows are often envisioned as 'highly energetic', in fact the flow regime is unrelated to the total amount of energy in a flow, and the Froude number represents a dimensionless ratio involving flow velocity and thickness (or kinetic over potential energy, Table 1, see e.g. Prave, 1990; Douillet, 2015). Thus, low-energy and waning conditions may be fully consistent with supercritical flows, and do not preclude any flow-regime interpretation. Possibly, PDCs might pass from subcritical to supercritical conditions on steep volcano flanks when decreasing their (under)flow thickness during a waning flow phase, together with a decrease in total energy of the current. Pyroclastic DBs might thus represent low-energy bedforms formed during the waning phase of a PDC into supercritical conditions.

ALTERNATIVE INTERPRETATIONS

Froude versus Reynolds

Whereas an important focus in the literature has been put on analyzing pyroclastic DBs in regard to the Froude number of formative flows, their growth patterns might actually be driven by the dynamics of turbulent structures, and thus reveal more about parameters such as the Reynolds number (indicative of the ratio of inertial to viscous forces internal to the flow) or the Strouhal number (indicative of the ratio of inertial forces due to local flow acceleration over those due to convective acceleration) than Froude number (Table 1; Douillet *et al.,* 2019). Particle-laden density currents are subjected to intermittency, pulsation and large turbulent fluctuations (e.g. Sequeiros *et al.,* 2018; Sovilla *et al.,* 2018). Pyroclastic currents may similarly be pulsating, characterized by high values of the Reynolds number (up to 6*10e9) and by large coherent turbulence structures up to hundreds of metres internally (e.g. Walker, 1984; Vazquez & Ort, 2006; Andrews & Manga, 2012; Lube *et al.,* 2015; Andrews, 2019; Brosch & Lube, 2020).

The vertical truncations observed in DB structures of type D, together with overturned truncation planes, have been reproduced experimentally by means of short-lived (<<1 s) air bursts (at 20 to 40 m s^{-1}; Douillet *et al.,* 2017, 2019). The origin of such short-lived pulses in a natural flow is unknown, but it could represent the signature of coherent turbulent structures in the basal portions of PDCs or the occurrence of fluctuating Froude jumps. Concurrently, extreme rates of sedimentation are needed to preserve steep to subvertical backset laminasets, since the

preservation of laminae with dip values well above the angle of repose in the sediment record implies rapid burial within a timespan of seconds. Interestingly, pulses of erosion and sedimentation waves are triggered by transient segregations of particles into mesoscale clusters around turbulent vortices (Burgisser *et al.,* 2005; Andrews & Manga, 2012; Breard *et al.,* 2016; Breard & Lube, 2017). It thus remains currently unclear whether pyroclastic DB structures of type D, but also B and C, can be explained by dynamics based on high Froude numbers or through a combination of turbulent fluctuations, high Reynolds numbers and high deposition rates.

Bed shape control – a flow-bed feedback

The predominance of individual bedforms rather than tabular sets, widespread occurrence of fully-aggrading DB structures (type B), and the general vertical stacking of DBs one above the other all point towards a strong spatial stability of pyroclastic DBs and towards an absence of migration (i.e. absence of translation of the entire structure). Such a spatial stability suggests that DBs are related to a bed configuration rather than a flow's free-surface. In parallel, Druitt (1992) noted that DB stratification nucleated against obstacles at Mount St. Helens, and the role of truncations in the nucleation and growth of backset bedding for DB structures of type C and D is illustrated here (Figs 7, 8, 11A and 12; see also Valentine *et al.,* 1989). Similarly, Allen (2001) attributes DBs to "internal waves generated by interaction with obstacles" and Freundt & Schmincke (1985) emphasized the role of topographic control in the emplacement of coarse-enriched backset beds. A simplistic equation framework also suggests that backset strata could grow in the supercritical regime as a simple feedback effect between an existing topography and the current, without being related to antidunes, chutes-and-pools or cyclic steps (Douillet, 2015). Additionally, several mechanisms of bed control for the growth of backset bedding unrelated to supercritical flows have been suggested, including differential draping, basal blocking, or the influence of local gradient on saltation (Douillet *et al.,* 2013b, 2014, 2019). Thus, there seems to be a fundamental role of the bed shape in the growth of backset beds, under supercritical conditions or otherwise. Whereas some initial bed configurations may be driven by supercritical flow dynamics, this seems largely contained in an erosive signal, or in low-angle structures. The vast majority of sediments deposited as pyroclastic DBs might be a sole consequence of these initial shapes and positive bed-flow feedback mechanisms.

CONCLUSIONS AND SUMMARY

Pyroclastic dune bedforms form peculiar sedimentary structures with widespread occurrence of fully-aggrading stratasets, steep truncations on stoss faces, and steep-sided backset beds. Since their recognition, these sedimentary structures have largely been associated with antidunes and chutes-and-pools, either as a descriptive term or an interpretation of flow dynamics, yet an understanding of their origin remains equivocal.

Here, it is stressed that backset stratification is not a sufficient feature for the attribution of such structures to supercritical flow conditions; likewise, foreset stratification is not a sufficient criterion to justify an interpretation of subcritical flow conditions. Most of the sedimentary signature of supercritical flows is likely represented by erosional truncations or low-angle bedforms. In that frame, an interpretation of low-angle bedforms as antidunes seems a possibility. Steep-sided backset-bearing structures similarly may represent a record of the subcritical 'pool' of Froude jumps, whereas associated underlying steep truncations would represent pulses of a retreating supercritical 'chute'. Cyclic steps seem rare to absent and, if present, they may be expressed as long-wavelength bedforms superimposed by metre-scale dune bedforms, or as repetitive trains of fully-aggrading, regressive structures. A prevalence of intermediate-stage structures (chutes-and-pools) over stable antidunes and cyclic steps could be attributed to the unstable and highly depositional nature of the flows. However questions remain to be addressed and alternative explanations are possible.

In an interpretation as Froude supercritical bedforms, the free flow interface shaping structures must be originated by a basal layer within a density-stratified current (i.e. flow stratification induced by vertical gradient in particle concentration). Thus, if the bedforms are interpreted as Froude supercritical, they would essentially inform about deposition under a thin, basal flow layer, providing little information about the majority of the overlying transport system. It is presently unclear whether such a density

interface is stable enough with regard to internal turbulence and buoyancy. The role of turbulent flow structures may also be fundamental in shaping truncations and backset beds, in particular when particles are segregated at the edge of mesoscale turbulent vortices. Turbulent cells and fluctuations alone may offer an alternative interpretation for the formation of pyroclastic structures unrelated to supercritical flows.

Independent of any possible interpretation in terms of flow regime, the bed-inherited shape also seems to play a fundamental role in the development of pyroclastic dune bedforms, which appears largely related to a flow–bed interaction process. Three explanations exist for the formation of backset stratification unrelated to supercritical flow conditions, all of them related to an existing topography as the trigger: (i) differential draping by suspended material; (ii) differential saltation capacity regulated by local gradient; and (iii) basal blocking of a bedload. Finally, most authors emphasize that pyroclastic bedforms are deposited under extremely high deposition rates, which is a central factor in the preservation of a variety of peculiar sedimentary structures observed in this kind of deposit, but so far unreported in clastic successions from other sedimentary environments.

ACKNOWLEDGEMENTS

Data was collected over numerous field campaigns, and short courses between 2009 and 2020, a PhD and post-doc project. I thank the two reviewers Benjamin Andrews and Martin Jutzeler as well as the editor Dario Ventra for their constructive reviews that improved the manuscript. U. Kueppers and D.B. Dingwell are acknowledged for continuous support over the years at LMU Munich and F. Schlunegger at University of Bern. Funding through several grants, including SNF-Ambizione, DFG-DO1953/1-1, DFG-KU2689/2-1, ERC Advanced Grant Evokes (247076), LMU-Excellent and ElitnetzwerkBayern. Numerous colleagues enabled great field work including A. Abolghassem, J. Battaglia, B. Bernard, B. Brand, J. Bustillos, J.R. Dujardin, C. Mato, D. Pacheco, N. Pollock, P. Rámon, R. Reschetizka, C. Robin, and È. Tsang-Hin-Sun, as well as the members of IG-EPN in Ecuador. The literature review would not have been possible without access through Sci-hub. Open Access funding enabled and organized by Projekt DEAL.

DATA AVAILABILITY STATEMENT

All images from the author. All figures available upon personal request. Length versus thickness data are available in the cited literrature.

REFERENCES

Alexander, J., **Bridge, J.S.**, **Cheel, R.J.** and **Leclair, S.F.** (2001) Bedforms and associated sedimentary structures formed under supercritical water flows over aggrading sand beds. *Sedimentology*, **48**(1), 133–152.

Allen, J.R.L. (1984). Development in sedimentology 30: Sedimentary structures their character and physical basis.

Allen, S.R. (2001) Reconstruction of a major caldera-forming eruption from pyroclastic deposit characteristics: Kos Plateau Tuff, eastern Aegean Sea. *J. Volcanol. Geoth. Res.*, **105**(1–2), 141–162.

Allen, S.R. and **Cas, R.A.F.** (1998) Rhyolitic fallout and pyroclastic density current deposits from a phreatoplinian eruption in the eastern Aegean Sea, Greece. *J. Volcanol. Geoth. Res.*, **86**, 219–251.

Andrews, B.J. (2019) Recognizing unsteadiness in the transport systems of dilute pyroclastic density currents. *Bull. Volcanol.*, **81**(2), 5.

Andrews, B.J. and **Manga, M.** (2012) Experimental study of turbulence, sedimentation, and coignimbrite mass partitioning in dilute pyroclastic density currents. *J. Volcanol. Geoth. Res.*, **225**, 30–44.

Belousov, A. and **Belousova, M.** (2001) Eruptive process, effects and deposits of the 1996 and ancient basaltic phreatomagmatic eruptions in Karymskoye lake, Kamchatka, Russia. *Spec. Publ. Int. Assoc. Sedimentol.*, **30**, 35–60.

Bestland, E.A. and **Krull, E.S.** (1999) Palaeoenvironments of Early Miocene Kisingiri volcano Proconsul sites: evidence from carbon isotopes, palaeosols and hydromagmatic deposits. *J. Geol. Soc.*, **156**(5), 965–976.

Boudet, J.F., **Amarouchene, Y.**, **Bonnier, B.** and **Kellay, H.** (2007) The granular jump. *J. Fluid Mech.*, **572**, 413–431.

Boudon, G., **Camus, G.**, **Gourgaud, A.** and **Lajoie, J.** (1993) The 1984 nuée-ardente deposits of Merapi volcano, Central Java, Indonesia: stratigraphy, textural characteristics, and transport mechanisms. *Bull. Volcanol.*, **55**(5), 327–342.

Boudon, G. and **Lajoie, J.** (1989) The 1902 Peléean deposits in the Fort Cemetery of St. Pierre, Martinique: a model for the accumulation of turbulent nuées ardentes. *J. Volcanol. Geoth. Res.*, **38**(1–2), 113–129.

Brand, B.D., **Bendaña, S.**, **Self, S.** and **Pollock, N.** (2016) Topographic controls on pyroclastic density current dynamics: insight from 18 May 1980 deposits at Mount St. Helens, Washington (USA). *J. Volcanol. Geoth. Res.*, **321**, 1–17.

Brand, B.D. and **Clarke, A.B.** (2009) The architecture, eruptive history, and evolution of the Table Rock Complex, Oregon: from a Surtseyan to an energetic maar eruption. *J. Volcanol. Geoth. Res.*, **180**(2–4), 203–224.

Brand, B.D., **Clarke, A.B.** and **Semken, S.** (2009) Eruptive conditions and depositional processes of Narbona Pass Maar volcano, Navajo volcanic field, Navajo Nation, New Mexico (USA). *Bull. Volcanol.*, **71**(1), 49.

Brand, B.D. and **Clarke, A.B.** (2012) An unusually energetic basaltic phreatomagmatic eruption: using deposit characteristics to constrain dilute pyroclastic density current dynamics. *J. Volcanol. Geoth. Res.*, **243**, 81–90.

Brand, B.D. and **Heiken, G.** (2009) Tuff cones, tuff rings, and maars of the Fort Rock-Christmas Valley basin, Oregon: exploring the vast array of pyroclastic features that record violent hydrovolcanism at Fort Rock and the Table Rock Complex. *Field Guides*, **15**, 521–538.

Brand, B.D. and **White, C.M.** (2007) Origin and stratigraphy of phreatomagmatic deposits at the Pleistocene Sinker Butte volcano, western Snake River Plain, Idaho. *J. Volcanol. Geoth. Res.*, **160**(3–4), 319–339.

Branney, M.J. and **Kokelaar, B.P.** (2002) *Pyroclastic Density Currents and the Sedimentation of Ignimbrites*, vol. **27**, Geological Society, London, Memoirs, London.

Breard, E.C., **Dufek, J.** and **Lube, G.** (2018) Enhanced mobility in concentrated pyroclastic density currents: an examination of a self-fluidization mechanism. *Geophys. Res. Lett.*, **45**(2), 654–664.

Breard, E.C., **Jones, J.R.**, **Fullard, L.**, **Lube, G.**, **Davies, C.** and **Dufek, J.** (2019) The permeability of volcanic mixtures —implications for pyroclastic currents. *J. Geophys. Res. Solid Earth*, **124**(2), 1343–1360.

Breard, E.C., **Lube, G.**, **Jones, J.R.**, **Dufek, J.**, **Cronin, S.J.**, **Valentine, G.A.** and **Moebis, A.** (2016) Coupling of turbulent and non-turbulent flow regimes within pyroclastic density currents. *Nat. Geosci.*, **9**(10), 767–771.

Breard, E.C. and **Lube, G.** (2017) Inside pyroclastic density currents–uncovering the enigmatic flow structure and transport behaviour in large-scale experiments. *Earth Planet Sci. Lett.*, **458**, 22–36.

Brennen, C.E., **Sieck, K.** and **Paslaski, J.** (1983) Hydraulic jumps in granular material flow. *Powder Technol.*, **35**(1), 31–37.

Brosch, E. and **Lube, G.** (2020) Spatiotemporal sediment transport and deposition processes in experimental dilute pyroclastic density currents. *J. Volcanol. Geoth. Res.*, **401**, 106946. https://doi.org/10.1016/j.jvolgeores.2020.106946

Brown, R.J. and **Branney, M.J.** (2004) Bypassing and diachronous deposition from density currents: evidence from a giant regressive bed form in the Poris ignimbrite, Tenerife, Canary Islands. *Geology*, **32**(5), 445–448.

Brown, R.J. and **Branney, M.J.** (2013) Internal flow variations and diachronous sedimentation within extensive, sustained, density-stratified pyroclastic density currents flowing down gentle slopes, as revealed by the internal architectures of ignimbrites on Tenerife. *Bull. Volcanol.*, **75**(7), 727.

Brown, R.J., **Kokelaar, B.P.** and **Branney, M.J.** (2007) Widespread transport of pyroclastic density currents from a large silicic tuff ring: the Glaramara tuff, Scafell caldera, English Lake District, UK. *Sedimentology*, **54**(5), 1163–1190.

Brown, R.J., **Orsi, G.** and **de Vita, S.** (2008) New insights into Late Pleistocene explosive volcanic activity and caldera formation on Ischia (southern Italy). *Bull. Volcanol.*, **70**(5), 583–603.

Bryan, S.E., **Cas, R.A.** and **Martı, J.** (1998) Lithic breccias in intermediate volume phonolitic ignimbrites, Tenerife (Canary Islands): constraints on pyroclastic flow depositional processes. *J. Volcanol. Geoth. Res.*, **81**(3–4), 269–296.

Burgisser, A. and **Bergantz, G.W.** (2002) Reconciling pyroclastic flow and surge: the multiphase physics of pyroclastic density currents. *Earth Planet Sci. Lett.*, **202**(2), 405–418.

Burgisser, A., **Bergantz, G.W.** and **Breidenthal, R.E.** (2005) Addressing complexity in laboratory experiments: the scaling of dilute multiphase flows in magmatic systems. *J. Volcanol. Geoth. Res.*, **141**(3–4), 245–265.

Burt, D.M., **Knauth, L.P.**, **Wohletz, K.H.** and **Sheridan, M.F.** (2008) Surge deposit misidentification at Spor Mountain, Utah and elsewhere: a cautionary message for Mars. *J. Volcanol. Geoth. Res.*, **177**(4), 755–759.

Cagnoli, B. and **Ulrych, T.J.** (2001) Ground penetrating radar images of unexposed climbing dune-forms in the Ubehebe hydrovolcanic field (Death Valley, California). *J. Volcanol. Geoth. Res.*, **109**(4), 279–298.

Carey, S.N. (1991) Transport and deposition of tephra by pyroclastic flows and surges. Sedimentation in Volcanic Setting. *SEPM Spec. Publ.*, **45**, 39–57.

Carling, P.A. and **Shvidchenko, A.B.** (2002) A consideration of the dune: antidune transition in fine gravel. *Sedimentology*, **49**(6), 1269–1282.

Carlson, R.H. and **Roberts, W.A.** (1963) *Project Sedan, Mass Distribution and Throwout Studies*. Boeing Company, Seattle, WA.

Cartigny, M.J., **Postma, G.**, **van den Berg, J.H.** and **Mastbergen, D.R.** (2011) A comparative study of sediment waves and cyclic steps based on geometries, internal structures and numerical modeling. *Mar. Geol.*, **280**(1–4), 40–56.

Cartigny, M.J., **Ventra, D.**, **Postma, G.** and **van Den Berg, J.H.** (2014) Morphodynamics and sedimentary structures of bedforms under supercritical-flow conditions: new insights from flume experiments. *Sedimentology*, **61**(3), 712–748.

Cas, R.A.F., **Van Otterloo, J.**, **Blaikie, T.N.** and **Van Den Hove, J.** (2017) The dynamics of a very large intra-plate continental basaltic volcanic province, the Newer Volcanics Province, SE Australia, and implications for other provinces. *Geol. Soc. Lond. Spec. Publ.*, **446**(1), 123–172.

Charland, A. and **Lajoie, J.** (1989) Characteristics of pyroclastic deposits at the margin of Fond Canonville, Martinique, and implications for the transport of the 1902 nuées ardentes of Mt. Pelée. *J. Volcanol. Geoth. Res.*, **38**(1–2), 97–112.

Chough, S.K. and **Sohn, Y.K.** (1990) Depositional mechanics and sequences of base surges, Songaksan tuff ring, Cheju Island, Korea. *Sedimentology*, **37**(6), 1115–1135.

Cizeau, P., **Makse, H.A.** and **Stanley, H.E.** (1999) Mechanisms of granular spontaneous stratification and segregation in two-dimensional silos. *Phys. Rev. E*, **59**(4), 4408.

Cole, P.D. (1991) Migration direction of sand-wave structures in pyroclastic-surge deposits: implications for depositional processes. *Geology*, **19**(11), 1108–1111.

Cole, P.D., **Calder, E.S.**, **Sparks, R.S.J.**, **Clarke, A.B.**, **Druitt, T.H.**, **Young, S.R.**, **Herd, R.A.**, **Harford, C.L.** and **Norton, G.E.** (2002) Deposits from dome-collapse and fountain-collapse pyroclastic flows at Soufrière Hills Volcano, Montserrat. *Geol. Soc. Lond. Memoirs*, **21**(1), 231–262.

Cole, P.D., **Guest, J.E.** and **Duncan, A.M.** (1993) The emplacement of intermediate volume ignimbrites: a case study from Roccamonfina Volcano, Southern Italy. *Bull. Volcanol.*, **55**(7), 467–480.

Cole, P.D., **Guest, J.E.**, **Duncan, A.M.** and **Pacheco, J.M.** (2001) Capelinhos 1957–1958, Faial, Azores: deposits formed by an emergent surtseyan eruption. *Bull. Volcanol.*, **63**(2–3), 204.

Cole, P.D. and **Scarpati, C.** (1993) A facies interpretation of the eruption and emplacement mechanisms of the upper part of the Neapolitan Yellow Tuff, Campi Flegrei, southern Italy. *Bull. Volcanol.*, **55**(5), 311–326.

Colella, A. and **Hiscott, R.N.** (1997) Pyroclastic surges of the Pleistocene Monte Guardia sequence (Lipari island, Italy): depositional processes. *Sedimentology*, **44**(1), 47–66.

Combe, G., **Richefeu, V.**, **Stasiak, M.** and **Atman, A.P.** (2015) Experimental validation of a nonextensive scaling law in confined granular media. *Phys. Rev. Lett.*, **115**(23), 238301.

Crowe, B.M. and **Fisher, R.V.** (1973) Sedimentary structures in base-surge deposits with special reference to cross-bedding, Ubehebe Craters, Death Valley, California. *Geol. Soc. Am. Bull.*, **84**(2), 663–682.

Dellino, P., **Isaia, R.** and **Veneruso, M.** (2004) Turbulent boundary layer shear flows as an approximation of base surges at Campi Flegrei (Southern Italy). *J. Volcanol. Geoth. Res.*, **133**(1–4), 211–228.

Dellino, P. and **La Volpe, L.** (2000) Structures and grain size distribution in surge deposits as a tool for modelling the dynamics of dilute pyroclastic density currents at La Fossa di Vulcano (Aeolian Islands, Italy). *J. Volcanol. Geoth. Res.*, **96**(1–2), 57–78.

Dietrich, P., **Ghienne, J.F.**, **Normandeau, A.** and **Lajeunesse, P.** (2016) Upslope-migrating bedforms in a proglacial sandur delta: cyclic steps from river-derived underflows? *J. Sediment. Res.*, **86**(1), 112–122.

Doronzo, D.M. and **Dellino, P.** (2014) Pyroclastic density currents and local topography as seen with the conveyer model. *J. Volcanol. Geoth. Res.*, **278**, 25–39.

Douillet, G.A. (2015). Flow and sedimentation of pyroclastic density currents: from large scale to boundary layer processes (Doctoral dissertation, Ludwig-Maximilians-Universität).

Douillet, G.A., **Bernard, B.**, **Bouysson, M.**, **Chaffaut, Q.**, **Dingwell, D.B.**, **Gegg, L.**, **Hoelscher, I.**, **Kueppers, U.**, **Mato, C.**, **Ritz, V.A.** and **Schlunegger, F.** (2019) Pyroclastic dune bedforms: macroscale structures and lateral variations. Examples from the 2006 pyroclastic currents at Tungurahua (Ecuador). *Sedimentology*, **66**(5), 1531–1559.

Douillet, G.A., **Bouysson, M.** and **Gegg, L.** (2017) Overturned strata in deposits of dilute pyroclastic density currents, field and analogue data. IAVCEI general Assembly.

Douillet, G.A., **Kueppers, U.**, **Mato, C.**, **Chaffaut, Q.**, **Bouysson, M.**, **Reschetizka, R.**, **Hoelscher, I.**, **Witting, P.**, **Hess, K.U.**, **Cerwenka, A.** and **Dingwell, D.B.** (2018) Revisiting the lacquer peels method with pyroclastic deposits: sediment plates, a precise, fine scale imaging method and powerful outreach tool. *J. Appl. Volcanol.*, **7**(1), 11.

Douillet, G.A., **Pacheco, D.A.**, **Kueppers, U.**, **Letort, J.**, **Tsang-Hin-Sun, È.**, **Bustillos, J.**, **Hall, M.**, **Ramón, P.** and **Dingwell, D.B.** (2013b) Dune bedforms produced by dilute pyroclastic density currents from the August 2006 eruption of Tungurahua volcano, Ecuador. *Bull. Volcanol.*, **75**(11), 762.

Douillet, G.A., **Rasmussen, K.R.**, **Kueppers, U.**, **Castro, D.L.**, **Merrison, J.P.**, **Iversen, J.J.** and **Dingwell, D.B.** (2014) Saltation threshold for pyroclasts at various bedslopes: Wind tunnel measurements. *J. Volcanol. Geoth. Res.*, **278**, 14–24.

Douillet, G.A., **Taisne, B.**, **Tsang-Hin-Sun, È.**, **Mueller, S.K.**, **Kueppers, U.** and **Dingwell, D.B.** (2015). Syn-eruptive, soft-sediment deformation of deposits from dilute pyroclastic density current: triggers from granular shear, dynamic pore pressure, ballistic impacts and shock waves.

Douillet, G.A., **Tsang-Hin-Sun, È.**, **Kueppers, U.**, **Letort, J.**, **Pacheco, D.A.**, **Goldstein, F.**, **Von Aulock, F.**, **Lavallée, Y.**, **Hanson, J.B.**, **Bustillos, J.** and **Robin, C.** (2013a) Sedimentology and geomorphology of the deposits from the August 2006 pyroclastic density currents at Tungurahua volcano, Ecuador. *Bull. Volcanol.*, **75**(11), 765.

Druitt, T.H. (1992) Emplacement of the 18 May 1980 lateral blast deposit ENE of Mount St. Helens, Washington. *Bull. Volcanol.*, **54**(7), 554–572.

Druitt, T.H. (1998) Pyroclastic density currents. *Geol. Soc. Lond. Spec. Publ.*, **145**(1), 145–182.

Druitt, T.H., **Avard, G.**, **Bruni, G.**, **Lettieri, P.** and **Maez, F.** (2007) Gas retention in fine-grained pyroclastic flow materials at high temperatures. *Bull. Volcanol.*, **69**(8), 881–901.

Dufek, J. (2016) The fluid mechanics of pyroclastic density currents. *Annu. Rev. Fluid Mech.*, **48**, 459–485.

Fierstein, J. and **Hildreth, W.** (2017) Eruptive history of the Ubehebe Crater cluster, Death Valley, California. *J. Volcanol. Geoth. Res.*, **335**, 128–146.

Fisher, R.V. (1977) Erosion by volcanic base-surge density currents: U-shaped channels. *Geol. Soc. Am. Bull.*, **88**(9), 1287–1297.

Fisher, R.V. (1990) Transport and deposition of a pyroclastic surge across an area of high relief: the 18 May 1980 eruption of Mount St. Helens, Washington. *Geol. Soc. Am. Bull.*, **102**(8), 1038–1054.

Fisher, R.V., **Schmincke, H.U.** and **Van Bogaard, P.** (1983) Origin and emplacement of a pyroclastic flow and surge unit at Laacher See, Germany. *J. Volcanol. Geoth. Res.*, **17**(1–4), 375–392.

Fisher, R.V. and **Waters, A.C.** (1969) Bed forms in base-surge deposits: Lunar implications. *Science*, **165**(3900), 1349–1352.

Fisher, R.V. and **Waters, A.C.** (1970) Base surge bed forms in maar volcanoes. *Am. J. Sci.*, **268**(2), 157–180.

Freundt, A. and **Schmincke, H.U.** (1985) Lithic-enriched segregation bodies in pyroclastic flow deposits of Laacher See volcano (East Eifel, Germany). *J. Volcanol. Geoth. Res.*, **25**(3–4), 193–224.

Gardner, J.E., **Andrews, B.J.** and **Dennen, R.** (2017) Liftoff of the 18 May 1980 surge of Mount St. Helens (USA) and the deposits left behind. *Bull. Volcanol.*, **79**(1), 8.

Gençalioğlu-Kuşcu, G., **Atilla, C.**, **Cas, R.A.** and **Kuşcu, İ.** (2007) Base surge deposits, eruption history, and depositional processes of a wet phreatomagmatic volcano in Central Anatolia (Cora Maar). *J. Volcanol. Geoth. Res.*, **159**(1–3), 198–209.

Giannetti, B. and **Luongo, G.** (1994) Trachyandesite scoria-flow and associated trachyte pyroclastic flow and surge at Roccamonfina Volcano (Roman Region, Italy). *J. Volcanol. Geoth. Res.*, **59**(4), 313–334.

Gilbert, G.K. (1914) The transportation of debris by running water (No. 86). US Government Printing Office.

Giordano, G., **Porreca, M.**, **Musacchio, P.** and **Mattei, M.** (2008) The Holocene Secche di Lazzaro phreatomagmatic succession (Stromboli, Italy): evidence of pyroclastic density current origin deduced by facies analysis and AMS flow directions. *Bull. Volcanol.*, **70**(10), 1221–1236.

Hoblitt, R.P. (1986). Observations of the eruptions of July 22 and August 7, 1980, at Mount St. Helens, Washington (Vol. 1335). US Government Printing Office.

Hoblitt, R.P., **Miller, C.D.** and **Vallance, J.W.** (1981) Origin and stratigraphy of the deposit produced by the May 18

directed blast. In *The 1980 Eruptions of Mount St. Helens, Washington* (Vol. **1250**, pp. 401–419). US Government Printing Office, Washington, DC.

Ito, M. (2010) Are coarse-grained sediment waves formed as downstream-migrating antidunes? Insight from an early Pleistocene submarine canyon on the Boso Peninsula, Japan. *Sed. Geol.*, **226**(1–4), 1–8.

Johnson, C.G. and **Gray, J.M.N.T.** (2011) Granular jets and hydraulic jumps on an inclined plane. *J. Fluid Mech.*, **675**, 87–116.

Jopling, A.V. and **Richardson, E.V.** (1966) Backset bedding developed in shooting flow in laboratory experiments. *J. Sediment. Res.*, **36**(3), 821–825.

Jordan, S.C., **Cas, R.A.F.** and **Hayman, P.C.** (2013) The origin of a large (>3 km) maar volcano by coalescence of multiple shallow craters: Lake Purrumbete maar, southeastern Australia. *J. Volcanol. Geoth. Res.*, **254**, 5–22.

Joyce, B. (2004). The young volcanic regions of southeastern Australia: early studies, physical volcanology and eruption risk. *Proc. R. Soc. Victoria*, **116**(1), 1–13.

Kelfoun, K., **Samaniego, P.**, **Palacios, P.** and **Barba, D.** (2009) Testing the suitability of frictional behaviour for pyroclastic flow simulation by comparison with a well-constrained eruption at Tungurahua volcano (Ecuador). *Bull. Volcanol.*, **71**(9), 1057.

Kennedy, J.F. (1963) The mechanics of dunes and antidunes in erodible-bed channels. *J. Fluid Mech.*, **16**(4), 521–544.

Lang, J., **Le Heron, D.P.**, **Van den Berg, J.H.** and **Winsemann, J.** (2021) Bedforms and sedimentary structures related to supercritical flows in glacigenic settings. *Sedimentology*, **68**, 1539–1579.

Le Roux, J. (2005) Comments on "Turbulent boundary layer shear flows as an approximation of base surges at Campi Flegrei (Southern Italy), by Dellino *et al.* (2004)". *J. Volcanol. Geoth. Res*, **141**, 331–332.

Love, D.W., **Gutjahr, A.** and **Lazari, A.** (2018) Sorting clasts across laminated maar dunes, Kilbourne and Hunts Holes, New Mexico: comparisons to sorting across aeolian and fluvial bedforms. *New Mex Geol.*, **40**(2), 45–60.

Lube, G., **Breard, E.C.**, **Cronin, S.J.**, **Procter, J.N.**, **Brenna, M.**, **Moebis, A.**, **Pardo, N.**, **Stewart, R.B.**, **Jolly, A.** and **Fournier, N.** (2014) Dynamics of surges generated by hydrothermal blasts during the 6 August 2012 Te Maari eruption, Mt. Tongariro, New Zealand. *J. Volcanol. Geoth. Res.*, **286**, 348–366.

Lube, G., **Breard, E.C.P.**, **Cronin, S.J.** and **Jones, J.** (2015) Synthesizing large-scale pyroclastic flows: experimental design, scaling, and first results from PELE. *J. Geophys. Res. Solid Earth*, **120**(3), 1487–1502.

Lube, G., **Breard, E.C.**, **Esposti-Ongaro, T.**, **Dufek, J.** and **Brand, B.** (2020) Multiphase flow behaviour and hazard prediction of pyroclastic density currents. *Nat. Rev. Earth Environ.*, **1**(7), 348–365.

Macıas, J.L., **Espındola, J.M.**, **Bursik, M.** and **Sheridan, M.F.** (1998) Development of lithic-breccias in the 1982 pyroclastic flow deposits of El Chichon volcano, Mexico. *J. Volcanol. Geoth. Res.*, **83**(3–4), 173–196.

Mackaman-Lofland, C., **Brand, B.D.**, **Taddeucci, J.** and **Wohletz, K.** (2014) Sequential fragmentation/transport theory, pyroclast size–density relationships, and the emplacement dynamics of pyroclastic density currents—a case study on the Mt. St. Helens (USA) 1980 eruption. *J. Volcanol. Geoth. Res.*, **275**, 1–13.

Makse, H.A., **Havlin, S.**, **King, P.R.** and **Stanley, H.E.** (1998). Spontaneous stratification in granular mixtures. arXiv preprint cond-mat/9809432.

Mandeville, C.W., **Carey, S.** and **Sigurdsson, H.** (1996) Sedimentology of the Krakatau 1883 submarine pyroclastic deposits. *Bull. Volcanol.*, **57**(7), 512–529.

Manville, V., **Németh, K.** and **Kano, K.** (2009) Source to sink: a review of three decades of progress in the understanding of volcaniclastic processes, deposits, and hazards. *Sed. Geol.*, **220**(3–4), 136–161.

Marshall, A., **Connor, C.**, **Kruse, S.**, **Malservisi, R.**, **Richardson, J.**, **Courtland, L.**, **Connor, L.**, **Wilson, J.** and **Karegar, M.A.** (2015) Subsurface structure of a maar–diatreme and associated tuff ring from a high-resolution geophysical survey, Rattlesnake Crater, Arizona. *J. Volcanol. Geoth. Res.*, **304**, 253–264.

Massari, F. (2017) Supercritical-flow structures (backset-bedded sets and sediment waves) on high-gradient clinoform systems influenced by shallow-marine hydrodynamics. *Sed. Geol.*, **360**, 73–95.

Mattson, P.H. and **Alvarez, W.** (1973) Base surge deposits in Pleistocene volcanic ash near Rome. *Bull. Volcanol.*, **37**(4), 553–572.

Mattsson, H.B. and **Tripoli, B.A.** (2011) Depositional characteristics and volcanic landforms in the Lake Natron-Engaruka monogenetic field, northern Tanzania. *J. Volcanol. Geoth. Res.*, **203**(1–2), 23–34.

McDonough, W.F., **Waibel, A.F.** and **Gannett, M.W.** (1984) The reinterpretation of Leone lake sediments as a pyroclastic surge deposit and its tectonic significance. *J. Volcanol. Geoth. Res.*, **20**(1–2), 101–115.

McPherson, J.G., **Flannery, J.R.** and **Self, S.** (1989) Comment on "Soft-sediment deformation (fluid escape) features in a coarse-grained pyroclastic surge deposit", north-central New Mexico. *Sedimentology*, **36**(5), 943–947.

Middleton, G.V. (1965) Antidune cross-bedding in a large flume. *J. Sediment. Res.*, **35**(4), 922–927.

Moore, J.G. (1967) Base surge in recent volcanic eruptions. *Bull. Volcanol.*, **30**(1), 337.

Moore, J.G., **Nakamura, K.** and **Alcaraz, A.** (1966) The 1965 eruption of Taal volcano. *Science*, **151**(3713), 955–960.

Moorhouse, B.L. and **White, J.D.** (2016) Interpreting ambiguous bedforms to distinguish subaerial base surge from subaqueous density current deposits. *Deposit. Rec.*, **2**(2), 173–195.

Németh, K., **Martin, U.** and **Harangi, S.** (2001) Miocene phreatomagmatic volcanism at Tihany (Pannonian Basin, Hungary). *J. Volcanol. Geoth. Res.*, **111**(1–4), 111–135.

Nocita, B.W. (1988) Soft-sediment deformation (fluid escape) features in a coarse-grained pyroclastic-surge deposit, north-central New Mexico. *Sedimentology*, **35**(2), 275–285.

Palladino, D.M. (2017) Simply pyroclastic currents. *Bull. Volcanol.*, **79**(7), 53.

Papale, P. and **Rosi, M.** (1993) A case of no-wind plinian fallout at Pululagua caldera (Ecuador): implications for models of clast dispersal. *Bull. Volcanol.*, **55**(7), 523–535.

Parejas, C.S., **Druitt, T.H.**, **Robin, C.**, **Moreno, H.** and **Naranjo, J.A.** (2010) The Holocene Pucón eruption of Volcán Villarrica, Chile: deposit architecture and eruption chronology. *Bull. Volcanol.*, **72**(6), 677–692.

Parker, G., **Ashworth, P.J.**, **Bennett, J.L.**, **Best, J.L.** and **McLelland, S.J.** (1996) Some speculations on the relation between channel morphology and channel-scale flow structures. Coherent flow structures in open channels, 423.

Pedrazzi, D., **Martí, J.** and **Geyer, A.** (2013) Stratigraphy, sedimentology and eruptive mechanisms in the tuff cone

of El Golfo (Lanzarote, Canary Islands). *Bull. Volcanol.*, **75** (7), 740.

Pope, E.L., **Jutzeler, M.**, **Cartigny, M.J.**, **Shreeve, J.**, **Talling, P.J.**, **Wright, I.C.** and **Wysoczanski, R.J.** (2018) Origin of spectacular fields of submarine sediment waves around volcanic islands. *Earth Planet Sci. Lett.*, **493**, 12–24.

Postma, G., **Kleverlaan, K.** and **Cartigny, M.J.** (2014) Recognition of cyclic steps in sandy and gravelly turbidite sequences, and consequences for the Bouma facies model. *Sedimentology*, **61**(7), 2268–2290.

Prata, G.S. (2012) *Complex Eruption Style and Deposit Changes During the Evolution of the Late Pleistocene Tower Hill Maarscoria Cone Volcanic Complex, Newer Volcanics Province, Victoria, Australia*. Monash University.

Prave, A.R. (1990) Clarification of some misconceptions about antidune geometry and flow character. *Sedimentology*, **37**(6), 1049–1052.

Radjai, F. and **Roux, S.** (2002) Turbulentlike fluctuations in quasistatic flow of granular media. *Phys. Rev. Lett.*, **89**(6), 064302.

Richards, A.F. (1959) Geology of the islas revillagigedo, mexico. *Bull. Volcanol.*, **22**(1), 73.

Rowley, P.D., **MacLeod, N.S.**, **Kuntz, M.A.** and **Kaplan, A.M.** (1985) Proximal bedded deposits related to pyroclastic flows of May 18, 1980, Mount St. Helens, Washington. *Geol. Soc. Am. Bull.*, **96**(11), 1373–1383.

Rowley, P.J., **Roche, O.**, **Druitt, T.H.** and **Cas, R.** (2014) Experimental study of dense pyroclastic density currents using sustained, gas-fluidized granular flows. *Bull. Volcanol.*, **76**(9), 855.

Sanders, J.E. (1960). Primary sedimentary structures formed by turbidity currents and related resedimentation mechanisms.

Scharff, L., **Hort, M.** and **Varley, N.R.** (2019) First in-situ observation of a moving natural pyroclastic density current using Doppler radar. *Sci. Rep.*, **9**(1), 1–9.

Schmincke, H.U., **Fisher, R.V.** and **Waters, A.C.** (1973) Antidune and chute and pool structures in the base surge deposits of the Laacher See area, Germany. *Sedimentology*, **20**(4), 553–574.

Schumacher, R. and **Schmincke, H.U.** (1991) Internal structure and occurrence of accretionary lapilli—a case study at Laacher See Volcano. *Bull. Volcanol.*, **53**(8), 612–634.

Scolamacchia, T. and **Schouwenaars, R.** (2009) High-speed impacts by ash particles in the 1982 eruption of El Chichón, Mexico. *J. Geophys. Res.*, **114**, B12206. https://doi.org/10.1029/2008JB005848

Scott, W.E., **Hoblitt, R.P.**, **Torres, R.C.**, **Self, S.**, **Martinez, M.M.L.** and **Nillos, T.** (1996) Pyroclastic flows of the June 15, 1991, climactic eruption of Mount Pinatubo. Fire and mud: Eruptions and lahars of Mount Pinatubo, Philippines, 545–570.

Self, S. and **Sparks, R.S.J.** (1978) Characteristics of widespread pyroclastic deposits formed by the interaction of silicic magma and water. *Bull. Volcanol.*, **41**(3), 196.

Self, S. and **Wright, J.V.** (1983) Large wave forms from the Fish Canyon Tuff, Colorado. *Geology*, **11**(8), 443–446.

Sequeiros, O.E., **Mosquera, R.** and **Pedocchi, F.** (2018) Internal structure of a self-accelerating turbidity current. *J. Geophys. Res. Oceans*, **123**(9), 6260–6276.

Sheridan, M.F. and **Updike, R.G.** (1975) Sugarloaf Mountain Tephra—a Pleistocene rhyolitic deposit of base-surge origin in northern Arizona. *Geol. Soc. Am. Bull.*, **86**(4), 571–581.

Sherwood, J., **Oyston, B.** and **Kershaw, A.P.** (2004). The age and contemporary environments of Tower Hill volcano, southwest Victoria, Australia. *Proc. R. Soc. Victoria*, **116** (1), 69–76.

Sigurdsson, H., **Carey, S.N.** and **Espindola, J.M.** (1984) The 1982 eruptions of El Chichón volcano, Mexico: stratigraphy of pyroclastic deposits. *J. Volcanol. Geoth. Res.*, **23**(1–2), 11–37.

Sigurdsson, H., **Carey, S.N.** and **Fisher, R.V.** (1987) The 1982 eruptions of El Chichón volcano, Mexico (3): physical properties of pyroclastic surges. *Bull. Volcanol.*, **49**(2), 467–488.

Simons, D.B., **Richardson, E.V.** and **Albertson, M.L.** (1961). Flume Studies Using Medium Sand (0.45 mm). *U.S. Geol. Survey Water-Supply Paper*, 1498-A.

Simons, D.B. and **Richardson, E.V.** (1966) Resistance to flow in alluvial channels. *U.S. Geol. Survey Prof. Paper*, **422-J**, J1–J61.

Slootman, A. and **Cartigny, M.J.** (2020) Cyclic steps: review and aggradation-based classification. *Earth Sci. Rev.*, **201**, 102949.

Smith, G.A. and **Katzman, D.** (1991) Discrimination of eolian and pyroclastic-surge processes in the generation of cross-bedded tuffs, Jemez Mountains volcanic field. *New Mex. Geol.*, **19**(5), 465–468.

Smith, G., **Rowley, P.**, **Williams, R.**, **Giordano, G.**, **Trolese, M.**, **Silleni, A.**, **Parsons, D.R.** and **Capon, S.** (2020) A bedform phase diagram for dense granular currents. *Nat. Commun.*, **11**(1), 1–11.

Smith, G.M., **Williams, R.**, **Rowley, P.J.** and **Parsons, D.R.** (2018) Investigation of variable aeration of monodisperse mixtures: implications for pyroclastic density currents. *Bull. Volcanol.*, **80**(8), 67.

Sohn, Y.K. (1997) On traction-carpet sedimentation. *J. Sediment. Res.*, **67**(3), 502–509.

Sohn, Y.K. and **Chough, S.K.** (1989) Depositional processes of the Suwolbong tuff ring, Cheju Island (Korea). *Sedimentology*, **36**(5), 837–855.

Sohn, Y.K. and **Park, K.H.** (2005) Composite tuff ring/cone complexes in Jeju Island, Korea: possible consequences of substrate collapse and vent migration. *J. Volcanol. Geoth. Res.*, **141**(1–2), 157–175.

Sovilla, B., **McElwaine, J.N.** and **Köhler, A.** (2018) The intermittency regions of powder snow avalanches. *J. Geophys. Res. Ser. F*, **123**(10), 2525–2545.

Sparks, R.S.J. (1976) Grain size variations in ignimbrites and implications for the transport of pyroclastic flows. *Sedimentology*, **23**(2), 147–188.

Sparks, R.S.J. and **Walker, G.P.L.** (1973) The ground surge deposit: a third type of pyroclastic rock. *Nat. Phys. Sci.*, **241**(107), 62–64.

Spinewine, B., **Sequeiros, O.E.**, **Garcia, M.H.**, **Beaubouef, R.T.**, **Sun, T.**, **Savoye, B.** and **Parker, G.** (2009) Experiments on wedge-shaped deep sea sedimentary deposits in minibasins and/or on channel levees emplaced by turbidity currents. Part II. Morphodynamic evolution of the wedge and of the associated bedforms. *J. Sediment. Res.*, **79**(8), 608–628.

Sulpizio, R. and **Dellino, P.** (2008) Sedimentology, depositional mechanisms and pulsating behaviour of pyroclastic density currents. *Dev. Volcanol.*, **10**, 57–96.

Sulpizio, R., **Mele, D.**, **Dellino, P.** and **La Volpe, L.** (2007) Deposits and physical properties of pyroclastic density currents during complex Subplinian eruptions: the AD

472 (Pollena) eruption of Somma-Vesuvius, Italy. *Sedimentology*, **54**(3), 607–635.

Suthren, R.J. (1985) Facies analysis of volcaniclastic sediments: a review. *Geol. Soc. London Spec. Publ.*, **18**(1), 123–146.

Tokunaga, T. and **Yokoyama, S.** (1979) Mode of eruption and volcanic history of Mukaiyama volcano, Nii-jima. *Geogr. Rev. Jpn*, **52**(3), 111–125.

Valentine, G.A. (1987) Stratified flow in pyroclastic surges. *Bull. Volcanol.*, **49**(4), 616–630.

Valentine, G.A. (2012) Shallow plumbing systems for small-volume basaltic volcanoes, 2: evidence from crustal xenoliths at scoria cones and maars. *J. Volcanol. Geoth. Res.*, **223**, 47–63.

Valentine, G.A., **Buesch, D.C.** and **Fisher, R.V.** (1989) Basal layered deposits of the Peach Springs Tuff, northwestern Arizona, USA. *Bull. Volcanol.*, **51**(6), 395–414.

Valentine, G.A. and **Giannetti, B.** (1995) Single pyroclastic beds deposited by simultaneous fallout and surge processes: Roccamonfina volcano, Italy. *J. Volcanol. Geoth. Res.*, **64**(1–2), 129–137.

Vallis, G.K. (2006) *Atmospheric and Oceanic Fluid Dynamics—Fundamentals and Large Scale Circulation*. Cambridge University Press, Cambridge, 745 pp. ISBN: 978-0- 521-84969-2.

Vazquez, J.A. and **Ort, M.H.** (2006) Facies variation of eruption units produced by the passage of single pyroclastic surge currents, Hopi Buttes volcanic field, USA. *J. Volcanol. Geoth. Res.*, **154**(3–4), 222–236.

Viroulet, S., **Baker, J.L.**, **Edwards, A.N.**, **Johnson, C.G.**, **Gjaltema, C.**, **Clavel, P.** and **Gray, J.M.N.T.** (2017) Multiple solutions for granular flow over a smooth two-dimensional bump. *J. Fluid Mech.*, **815**, 77–116.

Waitt, R.B., **Hansen, V.L.**, **Sarna-Wojcicki, A.M.** and **Wood, S.H.** (1981) Proximal air-fall deposits of eruptions (of Mount St. Helens) between May 24 and August 7, 1980-stratigraphy and field sedimentology. US Geological Survey Professional Paper, **1250**, 617–628.

Walker, G.P. (1971) Grain-size characteristics of pyroclastic deposits. *J. Geol.*, **79**(6), 696–714.

Walker, G.P. (1984) Characteristics of dune-bedded pyroclastic surge bedsets. *J. Volcanol. Geoth. Res.*, **20**(3–4), 281–296.

Walker, G.P.L., **Wilson, C.J.N.** and **Froggatt, P.C.** (1981) An ignimbrite veneer deposit: the trail-marker of a pyroclastic flow. *J. Volcanol. Geoth. Res.*, **9**(4), 409–421.

Walker, R.G. (1967) Upper flow regime bed forms in turbidites of the Hatch Formation, Devonian of New York State. *J. Sediment. Res.*, **37**(4), 1052–1058.

Waters, A.C. and **Fisher, R.V.** (1971) Base surges and their deposits: Capelinhos and Taal volcanoes. *J. Geophys. Res.*, **76**(23), 5596–5614.

Weit, A., **Roche, O.**, **Dubois, T.** and **Manga, M.** (2018) Experimental measurement of the solid particle concentration in geophysical turbulent gas-particle mixtures. *J. Geophys. Res. Solid Earth*, **123**(5), 3747–3761.

Wilson, C.J.N. (1985) The Taupo eruption, New Zealand. II. The Taupo ignimbrite. *Philos. Trans. R. Soc. London Ser. A Math. Phys. Sci.*, **314**(1529), 229–310.

Wilson, C.J. and **Hildreth, W.** (1998) Hybrid fall deposits in the Bishop Tuff, California: a novel pyroclastic depositional mechanism. *Geology*, **26**(1), 7–10.

Wohletz, K.H. (1998) Pyroclastic surges and two-phase compressible flows. From Magma to Tephra, 247–312.

Wohletz, K.H. and **Sheridan, M.F.** (1979) A model of pyroclastic surge. *Geol. Soc. Am. Spec. Pap.*, **180**, 177–194.

Wohletz, K.H., **Sheridan, M.F.** and **Brown, W.K.** (1989) Particle size distributions and the sequential fragmentation/transport theory applied to volcanic ash. *J. Geophys. Res. Solid Earth*, **94**(B11), 15703–15721.

Yokoyama, S. and **Tokunaga, T.** (1978) Base-surge deposits of Mukaiyama volcano, Nii-jima, Izu Islands. *Bull. Volcanol. Soc. Jpn*, **23**, 249–262.

Manuscript received 25 August 2020; revision accepted 16 February 2021